

Journal of Chemical Engineering and Material Science

Volume 8 Number 8 November 2017

ISSN 2141-6605



*Academic
Journals*

ABOUT JCEMS

The **Journal of Chemical Engineering and Materials Science (JCEMS)** is published monthly (one volume per year) by Academic Journals.

Journal of Chemical Engineering and Materials Science (JCEMS) is an open access journal that provides rapid publication (monthly) of articles in all areas of the subject such as semiconductors, high-temperature alloys, Kinetic Processes in Materials, Magnetic Properties of Materials, optimization of mixed materials etc.

The Journal welcomes the submission of manuscripts that meet the general criteria of significance and scientific excellence. Papers will be published shortly after acceptance. All articles published in JCEMS are peer-reviewed.

Contact Us

Editorial Office:

jcems@academicjournals.org

Help Desk:

helpdesk@academicjournals.org

Website:

<http://www.academicjournals.org/journal/JCEMS>

Submit manuscript online

<http://ms.academicjournals.me/>

Editors

Dr. R. Jayakumar

*Center for Nanosciences Amrita
Institute of Medical Sciences and Research
Centre
Amrita Vishwa Vidyapeetham University
Cochin-682 026
India*

Prof. Lew P Christopher

*Center for Bioprocessing Research and
Development(CBRD)
South Dakota School of Mines and
Technology(SDSM&T)
501 East Saint Joseph Street
Rapid City 57701 SD
USA*

Prof. Huisheng Peng

*Laboratory of Advanced Materials
Department of Macromolecular Science
Fudan University Shanghai 200438
China*

Prof. Layioye Ola Oyekunle

*Department of Chemical Engineering
University of Lagos Akoka-Yaba
Lagos Nigeria*

Dr. Srikanth Pilla

*Structural Engineering and Geomechanics Program
Dept of Civil and Environmental Engineering
Stanford University
Stanford CA 94305-4020
USA.*

Asst Prof. Narendra Nath Ghosh

*Department of Chemistry,
Zuarinagar, Goa-403726,
India.*

Dr. Rishi Kumar Singhal

*Department of Physics, University of Rajasthan,
Jaipur 302055 India.*

Dr. Daoyun Song

*West Virginia University
Department of Chemical Engineering,
P. O Box 6102, Morgantown, WV 26506,
USA.*

Editorial Board

Prof. Priyabrata Sarkar

*Department of Polymer Science and
Technology University of Calcutta
92 APC Road Kolkata India*

Dr. Mohamed Ahmed AbdelDayem

*Department of Chemistry
College of Science King Faisal University
Al-Hasa Saudi Arabia*

Ayo Samuel Afolabi

*School of Chemical and Metallurgical
Engineering
University of the Witwatersrand Johannesburg
Private Bag 3 Wits 2050 Johannesburg South
Africa*

Dr. S. Bakamurugan

*Institut für Anorganische und Analytische
Chemie Universität Münster Corrensstrasse
30 D-48149 Münster Germany*

Prof. Esezobor David Ehigie

*Department of Metallurgical and Materials
Engineering Faculty of Engineering
University of Lagos, Lagos*

Dr sunday ojolo

*Mechanical Engineering Department
University of Lagos
Akoka Lagos, Nigeria*

Prof. Dr. Qingjie Guo

*College of Chemical Engineering
Qingdao University of Science and Technology
Zhengzhou 53 Qingdao 266042 China*

Dr Ramli Mat

*Head of Chemical Engineering Department
Faculty of Chemical and Natural Resources
Engineering Universiti Teknologi
Malaysia*

Prof. Chandan Kumar Sarkar

*Electronics and Telecommunication Engineering
Jadavpur University Kolkata India*

Dr.-Ing. Ulrich Teipel

*Georg-Simon-Ohm Hochschule Nürnberg
Mechanische Verfahrenstechnik/
Partikeltechnologie Wassertorstr. 10
90489 Nürnberg Germany*

Dr. Harsha Vardhan

*Department of Mining Engineering
National Institute of Technology Karnataka Surathkal
P.O - Srinivasnagar - 575025 (D.K)
Mangalore Karnataka State India*

Dr. Ta Yeong Wu

*School of Engineering
Monash University Jalan Lagoon
Selatan Bandar Sunway 46150
Selangor Darul Ehsan Malaysia*

Dr. Yong Gao

*DENTSPLY Tulsa Dental Specialties
5100 E. Skelly Dr. Suite 300
Tulsa Oklahoma USA*

Dr. Xinli Zhu

*School of chemical Biological and materials
engineering the University of Oklahoma
100 E Boyd St SEC T-335 Norman, OK 73019
USA*

ARTICLES

Fatigue life prediction of unidirectional carbon fiber/epoxy composite on Mars 74
A. Anvari

Thermal fatigue life of carbon nanotube wire and unidirectional carbon fiber/epoxy composite (UCFEC) in earth orbit 101
A. Anvari

Full Length Research Paper

Fatigue life prediction of unidirectional carbon fiber/epoxy composite on Mars

A. Anvari

Department of Mechanical and Aerospace Engineering, University of Missouri-Columbia, Columbia, Missouri, U.S.A.

Received 23 July, 2017; Accepted 11 August, 2017

In the presented study, by applying analytical methods and using experimental data, equations are achieved to predict the fatigue life of unidirectional carbon fiber/epoxy composite (UCFEC) that is applied in aerospace structures. The experimental data used to obtain these equations are achieved by low earth orbit (LEO) environment simulation experiment and other experiments. By employing convex curves analytical method, some equations to predict the fatigue life of unidirectional carbon fiber/epoxy composite in LEO are achieved. Then, by inspiration of convex curves method, steady-linear method to predict the fatigue life of unidirectional carbon fiber/epoxy composite on Mars is proposed. Furthermore, the results of convex curves method have proved that the main factor causing fracture of UCFEC in vacuum thermal cycles is the degradation of inter laminar shear strength between the carbon fiber and epoxy. Finally, the results obtained by these methods are compared with the results from other experiments of composite materials. The comparison showed that the results of this study seem acceptable.

Key words: Fatigue life prediction, unidirectional carbon fiber, composite, earth orbit, Mars.

INTRODUCTION

Mars

Planet Mars has been the centre of attention for many scientists and people due to its reddish colour and the possibility of existing life on this planet (Pasachoff, 1993). Mars is a small planet, 6800 km across, which is only about half the diameter and one-eighth the volume of Earth or Venus, although somewhat larger than Mercury. Mars's atmosphere is thin-at the surface with its pressure only 1% of the surface pressure of Earth's atmosphere; however, it might be sufficient for certain kinds of life. It turns out to be 24 h 37 min 22.6 s from one Martian

noontime to the next, so a day on Mars lasts nearly the same length of time as a day on Earth. Mars revolves around the sun in 23 Earth months. Surface temperatures measured from the landers ranged from a low of 150K at the northern site of lander 1 to over 300K at lander 2. Temperature varied each day by 35 to 50°C (Pasachoff, 1993).

Human missions to Mars have been studied by many authors (Salotti, 2011, 2012). Likelihood of vehicular mission-success-and-safety is investigated by Suhir (2012). The Mars500 mission was a 520-day long simulation of a round trip to Mars. After going through an

E-mail: aabm9@mail.missouri.edu.

Author(s) agree that this article remain permanently open access under the terms of the [Creative Commons Attribution License 4.0 International License](https://creativecommons.org/licenses/by/4.0/)



Figure 1. Surface activity documented from orbit includes avalanches, spiders carved by carbon dioxide and a dust devil 800 m tall (top to bottom) (McEwen, 2013).

intense selection process, 6 individuals from various countries lived and worked for several months in a pressurized facility in Moscow, Russia, mimicking as close as possible the conditions of real space flight. The simulation concluded in November 2011 when the crew came out of the facility in seemingly good health and mood (Diego and Charles, 2014). Conceptual study of Mars Aero-flyby Sample Collection (MASC) is conducted as part of the next Mars exploration mission currently entertained in Japan Aerospace Exploration Agency (Fujita et al., 2014). Some major risks-of-failure issues for the future manned missions to Mars are discussed, with an objective to address criteria for making such missions possible, successful, safe and cost-effective (Salotti and Suhir, 2014).

Water on Mars

It seems that water is essential for existing life for every creature on Earth due to sustaining metabolism and

cellular structure stability (Des Marias, 2010). A student in the laboratory discovered a perplexing feature of Mars's surface that had never been seen before- streaks across the surface, flowing downhill, that grow slowly and change with the seasons in ways that suggest they are flows of liquid water (Figure 1; McEwen, 2013). Photographs from the Phoenix mission showed what looked like water droplets on the legs of the robotic lander (McEwen, 2013). Frost deposits observed occasionally only at the Viking-2 lander site (48°N, 226°W) on Mars (Mohlmann and Thomsen, 2011).

A one-way human mission to Mars

It sounds like Mars is the most similar planet to Earth due to its moderate surface gravity, atmosphere, and existing water and carbon dioxide. Therefore, it may be considered as a second home of human in solar system. After Venus, Mars is the nearest planet to Earth and trip to Mars takes about six months according to recent

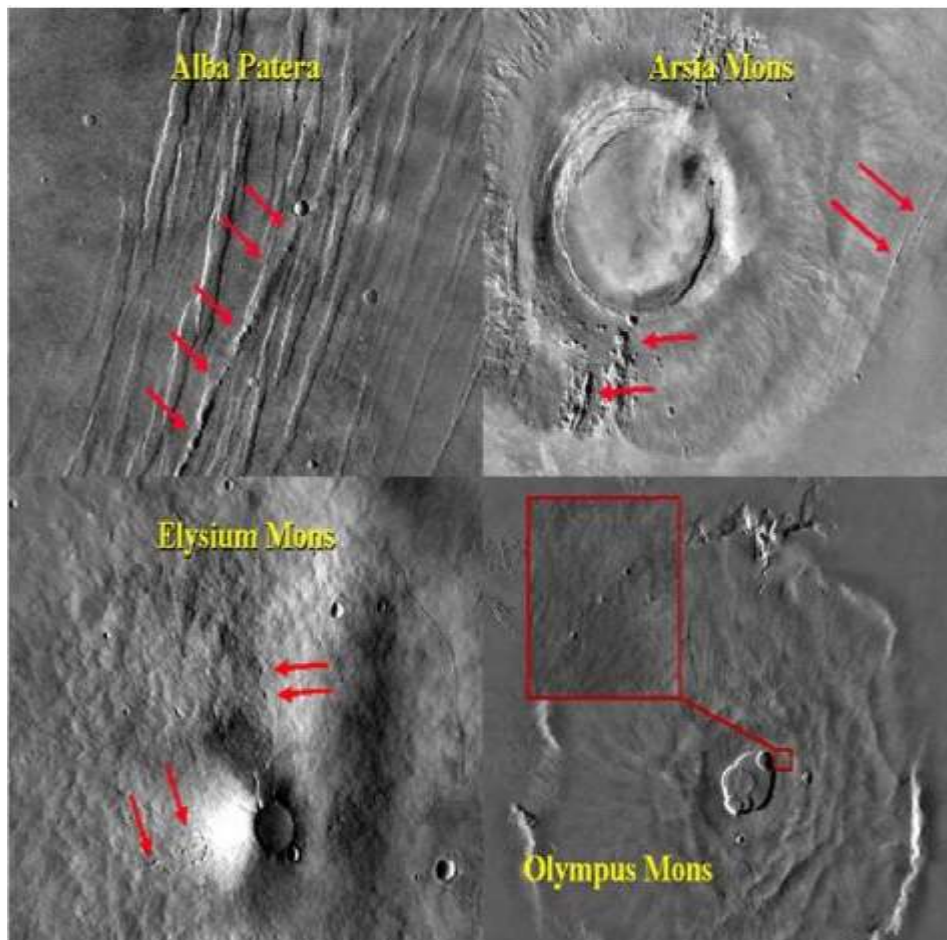


Figure 2. Collapsed lava tubes on Mars highlighted by arrows (composite image provided by R.D. Gus Frederick, Silverton, Oregon, based on data from NASA) (Schulze-Makuch and Davies, 2010).

space technology (Schulze-Makuch and Davies, 2010).

The astronauts would go to Mars with the intention of staying for the rest of their lives, as trailblazers of a permanent human Mars colony. They would be resupplied periodically from Earth, and eventually develop some home grown industry such as food production and mineral/chemical processing. Their role would be to establish a base camp (Figure 2) to which more colonists would eventually be sent, and to carry out important scientific and technological projects in the interim (Schulze-Makuch and Davies, 2010).

Over time, the human contingent on Mars would slowly increase with follow-up missions. Several cave-centered biospheres would be created, each being in constant communication with other cave-centered biospheres to share experiences on which approaches are working best. At some later time, probably several decades after the first human mission, the colony's population might have expanded to about 150 individuals, which would constitute a viable gene pool to allow the possibility of a successful long-term reproduction program. New arrivees

and possibly the use of genetic engineering would further enhance genetic variety and contribute to the health and longevity of the colonists (Schulze-Makuch and Davies, 2010).

Carbon fiber/epoxy composite

It appears that since 1930s polymers have been used in different applications like clothing, carpets, ropes, and reinforcing due to its versatile forms like films, fibers, sheets, and coatings (Song et al., 2013). Composites are materials widely used lately in the aeronautical industry to manufacture several parts as flaps, aileron, landing-gear doors and others. Polymer matrix composite materials constituted by continuous carbon fibers embedded in a thermosetting epoxy resin were first developed to satisfy high standards required in aircraft design. Compared to metals, the epoxy/carbon composites offer similar or better mechanical properties by mixing in these two distinct phases, fibers and resin, and adopting different

fiber configurations (Voicu, 2012). As a contribution to this field of study, development and mechanical properties of carbon fibre reinforced EP/VE hybrid composite systems is performed by Meszaros and Turcsan (2014).

Fatigue, damage, and fracture

In order to accurately determine the fatigue life of composites, some factors are required to be considered. These factors may include; stress amplitude, mean stress, and frequency and waveform of stress cycling during service (Hertzberg, 1989; Sendekyj, 1990; Harris, 2003).

In application of theories for fatigue, damage, and fracture, determination of stress intensity factors in half-plane containing several moving cracks is investigated by Malekzadeh Fard et al. (2013). Basic solutions of multiple parallel symmetric mode-III cracks in functionally graded piezoelectric/piezomagnetic material plane is proposed by Pan et al. (2013), while nonlinear progressive damage model for composite laminates used for low-velocity impact is evaluated by Guo et al. (2013). In addition, recent technique for thermal-fatigue simulation of heat-resistant steels is provided by Biro and Csizmadia (2012). Furthermore, in the area of obtaining the analytical evaluation methods of materials' properties, a few works are submitted by Anvari (2014, 2016, 2017; Adibnazari and Anvari, 2017).

Advanced carbon fiber-reinforced composite laminates have been widely used in satellite structures, where the advantages of these materials- their high specific stiffness, near-zero coefficients of thermal expansion (CTE) and dimensional stabilities make them uniquely suited for applications in a low-specific-weight environment. However, since the beginning of composite structure applications, there has been a strong need to quantify the environmental effects on the composite materials based on the coupon-level laminate test data. Recent studies have shown that the environmental conditions that are the most representative of space and that tend to degrade the properties of composite laminates involve vacuum, thermal cycling atomic oxygen (AO) and micrometeoroid particles. In this respect, there is significant interest in the construction of an experimental database to capture the collective understanding of the degradation mechanisms of composite laminate in in-service environments. It is necessary to be able to predict the long-term durability of composite laminates with engineering accuracy to use these materials with confidence in critical load-bearing structures (Park et al., 2012).

One of environmental effects of space known to induce environmental degradation is thermal cycling because a satellite in low earth orbit (LEO, between 100 and 1500 km above the earth's surface) passes in and out of the earth's shadow. The exterior surface is exposed to long-term periodic sharp temperature changes as a result.

This type of non-mechanical fatigue is of significant concern for the design of composite laminates because of the strong anisotropy of the thermoelastic characteristics of the long-fiber unidirectional plies. Considering the importance of the vacuum thermal cycling, several studies have been conducted in this area. Gao et al. (2005); Shin et al (2000); Funk and Sykes (1989) in particular have focused on the fundamental understanding of cumulative damage development due to cyclic exposure. However, such research should be expanded. The limited number of thermal cycles (350 cycles or less) used in their studies should be expanded to draw a definite conclusion, and studying the effects of thermal cycling on more representative space-grade materials for LEO application combined in series with mechanical assessments is required to assess the long-term durability issues of these materials (Park et al., 2012).

In the presented research, the effect of thermal cyclic exposures on unidirectional carbon fiber/epoxy composite (UCFEC) in Mars environment is investigated. Carbon fiber/epoxy composite is a candidate material applied in aerospace structures which might be deployed in LEO or land on Mars. The cumulative degradation effects on modulus and mechanical strength for UCFEC due to thermal cyclic exposures is considered and calibrated to predict the fatigue life in Mars environment. These data are obtained from the simulation of LEO environment in laboratory (Park et al., 2012) and another experiment (Nakamura et al., 2007). In this study, by applying analytical methods and using the experimental data, equations and methods to obtain the fatigue life of UCFEC in LEO and Mars environments are achieved.

EXPERIMENTAL PROCEDURES

The thermal cycling tests were conducted using a thermal vacuum chamber (Hanchang Eng, South Korea), as shown in Figure 3A (Park et al., 2012). The experiment was performed in an environmental chamber with a proportional integral derivative (PID) programmable temperature controller. Test temperature range should be as large and practicable to meet environmental stress screening (ESS) purposes based on the guideline in MIL-STD-810F and MIL-STD1540C. It is generally required to reveal potential flaws in material exposed to more extreme temperature change condition. In this study, extreme temperature conditions (120 to -175°C) encompass an environmental severity over that expected during service life based on the previous studies. Common to each of the thermal cycling profiles, low temperature ($T_{low} = -175 \pm 5^\circ\text{C}$) simulates the solar eclipse condition and cycle-specific high temperature ($T_{high} = 120 \pm 5^\circ\text{C}$) corresponds to the sun illumination for each 2 min duration time, as shown in Figure 3B (Park et al., 2012). Following this profile, one cycle was designed as the sequence from 120 to -175°C and back to 120°C so that the total duration of each cycle was approximately 43 min. A vacuum pressure of 1.3^{-3} Pa was employed throughout the thermal cycling test (Park et al., 2012).

The extent of degradation was determined experimentally by exposing the test panels to vacuum thermal cycling. The experiments were repeated for 500 cycles (358 h), 1000 cycles (716 h), 1500 cycles (1074 h) and 2000 cycles (1432 h). Following the

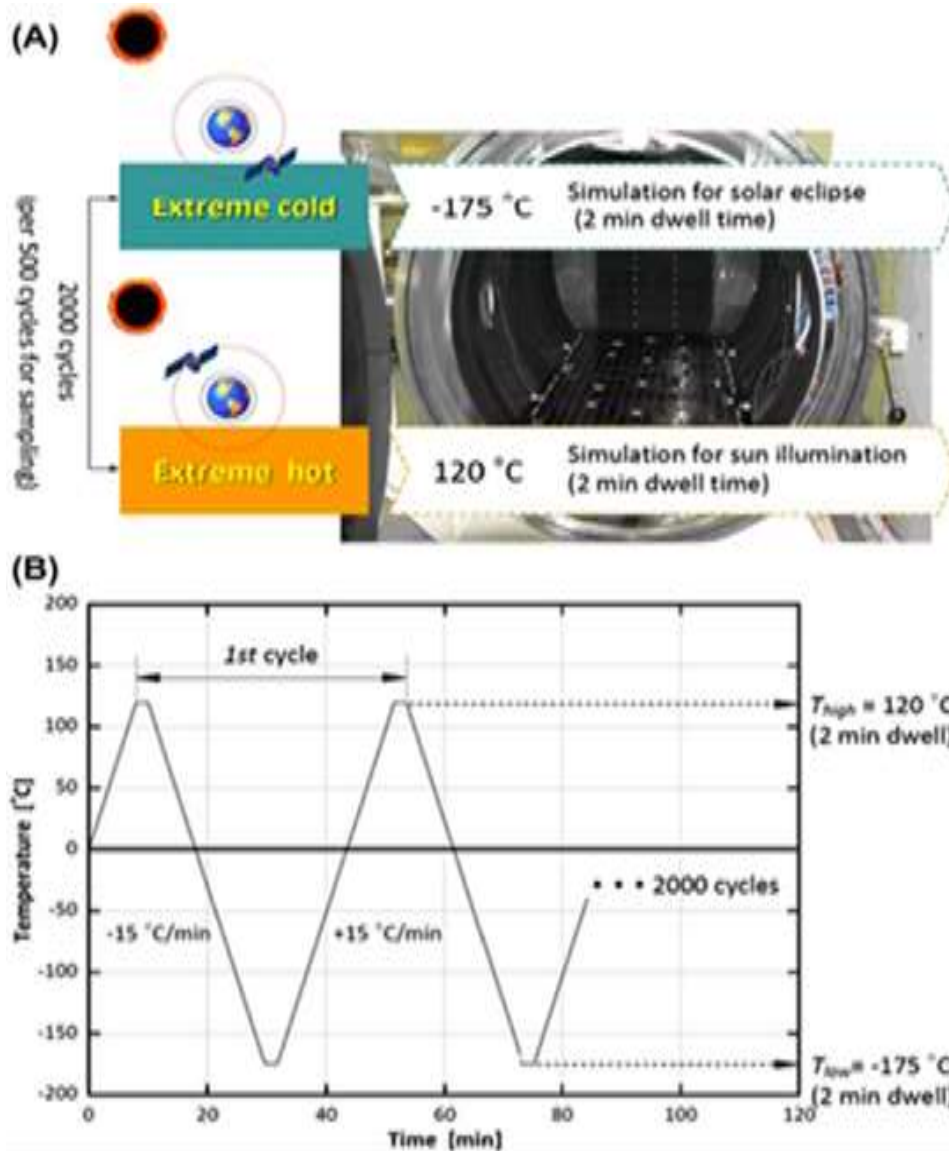


Figure 3. Vacuum thermal cycling test for the LEO space environment simulation: (A) thermal vacuum chamber; and (B) thermal cycling temperature profiles (Park et al., 2012).

thermal cycling exposure, all partly-or fully-aged test panels were cut into the desired dimensions using a water-cooled diamond saw and subsequently dried in a vacuum oven at 60°C for 24 h to remove moisture after the cutting operation. Series of physical and mechanical tests were then performed in the standard laboratory atmosphere of $23 \pm 2^\circ\text{C}$ and $50 \pm 5\%$ rh on the baseline (unaged) and environmentally conditioned test samples (Park et al., 2012).

In Figure 4 (Park et al., 2012), the sample of UCFEC used in simulation experiment in LEO environment is shown. In the following parts of this study, by the existing assumption in LEO environment and material properties of UCFEC, crack density growth rate can be obtained. In Table 1, the material properties of UCFEC are indicated.

PROBLEM FORMULATION

In this part of the research, equations that are used to obtain the

relation for estimating the fatigue life of UCFEC in LEO environment simulation experiment and Mars environment are introduced. In the Equations 2 to 17 (Liu and Nairn, 1990), E_A and E_T are the axial and transverse moduli of the carbon fiber, E_C is the modulus of the epoxy laminate, T_s is the specimen temperature, while T_0 is the temperature when the laminate is uncracked and at the stress free temperature. E_0 is

$$E_0 = (E_A + E_C) / 2, \quad (1)$$

$\Delta\alpha = \alpha_T - \alpha_A$ (the difference between the transverse and longitudinal thermal expansion coefficients of carbon fiber). $T = T_s - T_0$. Finally, p , q , and the constants C_1 to C_4 are functions of the mechanical properties and thicknesses of the plies: t_1 is half thickness of epoxy, t_2 is the thickness of carbon fiber, and $h = t_1 + t_2$ as shown in Figure 5 (Liu and Nairn, 1990).

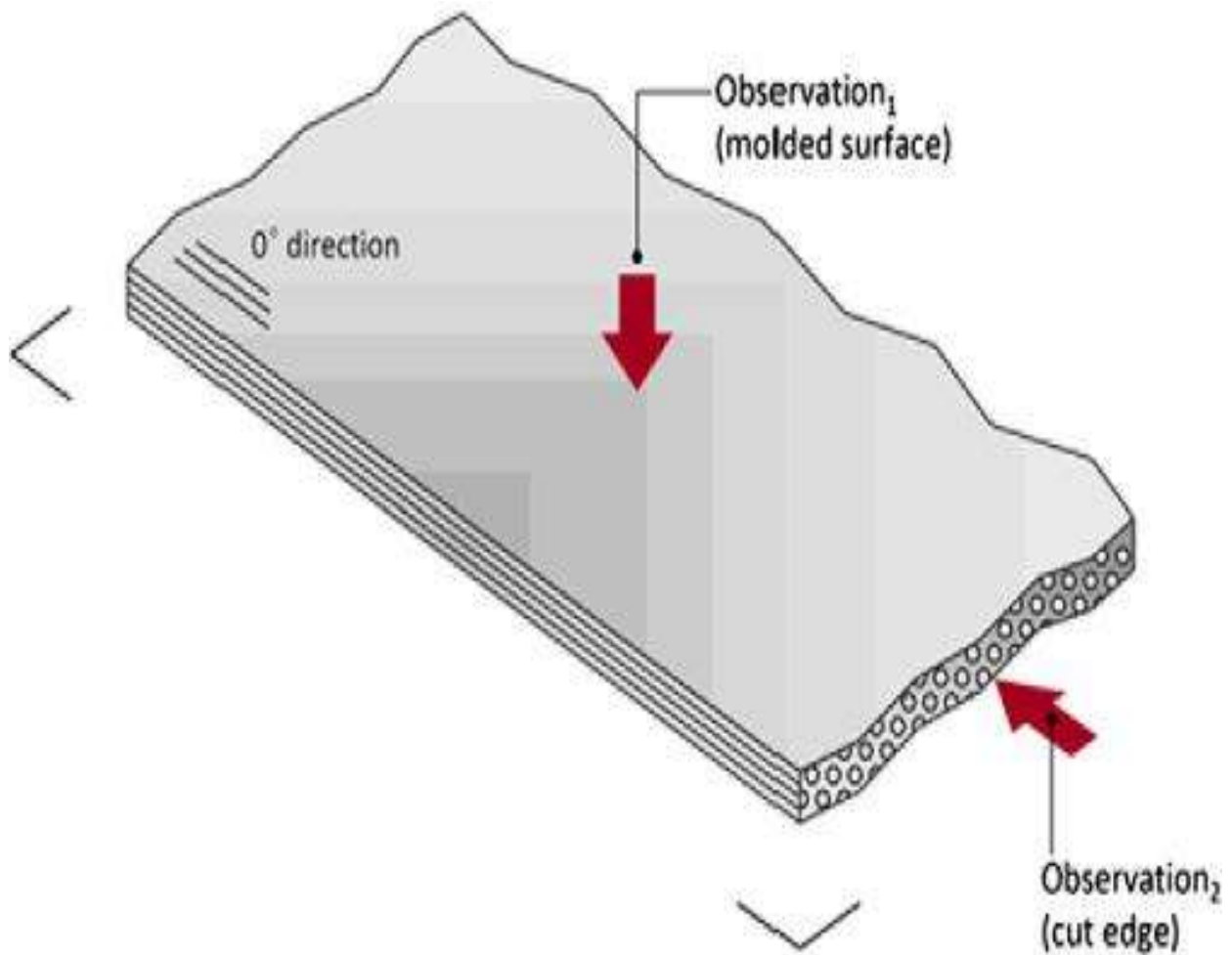


Figure 4. Microscopic observation of unidirectional carbon fiber/epoxy laminates exposed to vacuum thermal cycling (Park et al., 2012).

Table 1. Material properties of UCFEC (Park et al., 2012; Karadeniz and Kumlutas, 2007).

Materials	Epoxy	Carbon Fiber
Axial Coefficient of Thermal Expansion (1/°C)	43.92e-6	-0.83e-6
Transverse Coefficient of Thermal Expansion (1/°C)	43.92e-6	6.84e-6
Axial Poisson's ratio	0.37	0.2
Transverse Poisson's ratio	0.37	0.4
Axial Elastic Modulus (GPa)	4.35	377
Transverse Elastic Modulus (GPa)	4.35	6.21
Axial Shear Modulus (GPa)	1.59	7.59
Transverse Shear Modulus (GPa)	1.59	2.21
Thickness (mm)	0.5	0.5

G_A , G_T , ν_A , and ν_T , are the axial and transverse shear moduli and Poisson's ratio, respectively, while G_c is epoxy shear modulus. Note that the above solution is specific for $4q/p^2 > 1$.

$$C_1 = \frac{hE_0}{t_2 E_A E_T}, \tag{2}$$

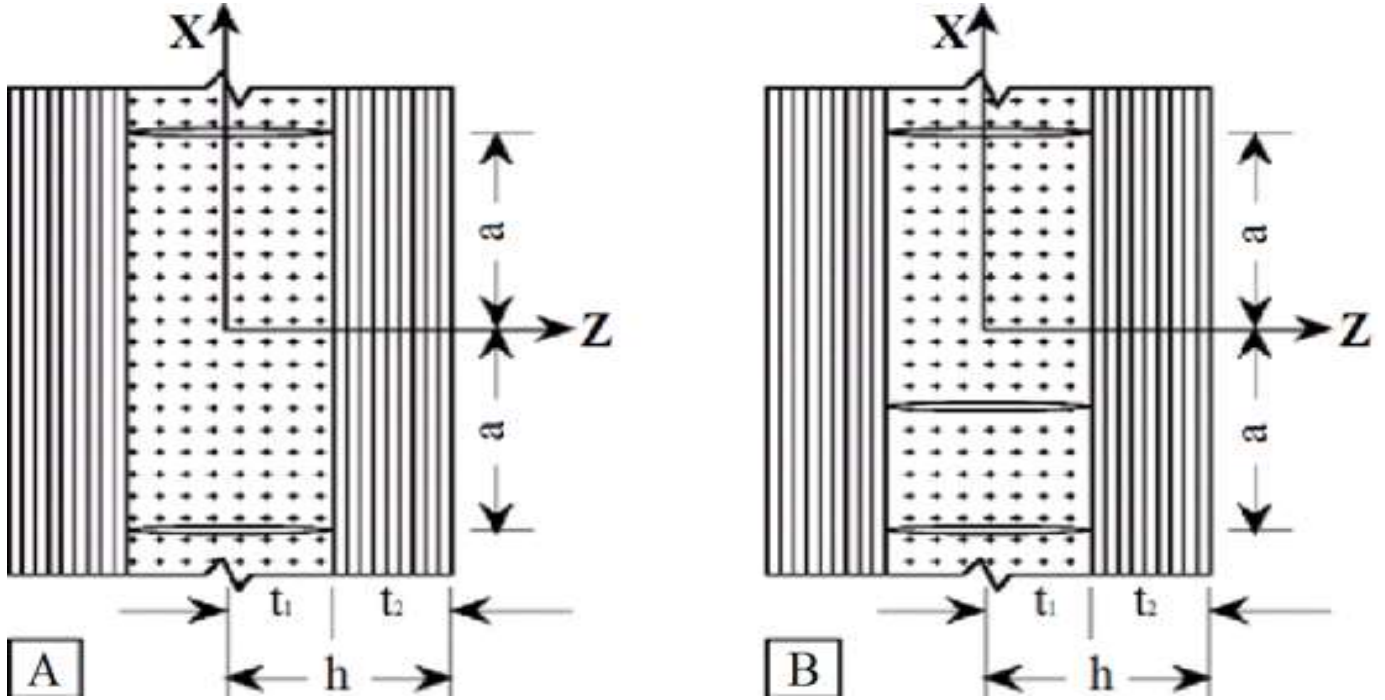


Figure 5. Edge view of UC FEC with microcracks. A: Two microcracks. B: The formation of a new microcrack (Liu and Nairn, 1990).

$$C_2 = \frac{v_T}{E_T} \left(\lambda + \frac{2}{3} \right) - \frac{\lambda v_d}{3E_A}, \quad (3)$$

$$\lambda = t_1 / t_2, \quad (4)$$

$$C_3 = \frac{\lambda + 1}{60E_T} (3\lambda^2 + 12\lambda + 8), \quad (5)$$

$$C_4 = \frac{1}{3} \left(\frac{1}{G_T} + \frac{\lambda}{G_A} \right). \quad (6)$$

By applying C_1 to C_4 , p and q are obtained.

$$p = (C_2 - C_4) / C_3, \quad (7)$$

$$q = C_1 / C_3. \quad (8)$$

By employing p and q , α and β are achieved.

$$a = \frac{1}{2} \sqrt{2\sqrt{q} - p}, \quad (9)$$

$$b = \frac{1}{2} \sqrt{2\sqrt{q} + p}. \quad (10)$$

In Tables 2 and 3, the numerical values obtained by the above

equations are indicated.

In Figure 6, $B = 2h$ is the total thickness, W is the sample width (y -direction dimension), and L is the sample length (x -direction dimension). In this research, as shown in Figure 6, $B = 1$ mm, $W = 5$ mm, and $L = 25$ mm. With the present assumption, the numerical values in the paper, and Table 1, the numerical values in Table 2 are obtained.

The new function $\chi(\rho)$ for $4q/p^2 > 1$ is

$$\chi(\rho) = 2\alpha\beta(\alpha^2 + \beta^2) \frac{\cosh 2\alpha\rho - \cos 2\beta\rho}{\beta \sinh 2\alpha\rho + \alpha \sin 2\beta\rho}, \quad (11)$$

$$\rho = a/t_1. \quad (12)$$

$$G_m = \left(\frac{E_T}{E_c} \sigma_0 - \frac{\Delta\alpha T}{C_1} \right)^2 C_3 t_1 Y(D), \quad (13)$$

where G_m is energy release rate and $Y(D)$ is a calibration function that depends on the crack density, D . The calibration function is therefore (Anvari, 2017)

$$Y(D) = 2\chi(\rho/2) - \chi(\rho). \quad (14)$$

$$\frac{dD}{dV} = \Delta\Delta G_m^n, \quad (15)$$

so, before the crack forms

$$D = N_c / L, \quad (16)$$

Table 2. The numerical values that are obtained from the equations.

C_1	C_2	C_3	C_4
0.12e-9	0.17e-9	0.35e-9	0.24e-9

Table 3. The numerical values that are obtained from the equations.

λ	p	q	α	β
2	-0.1899	0.345	0.584	0.496

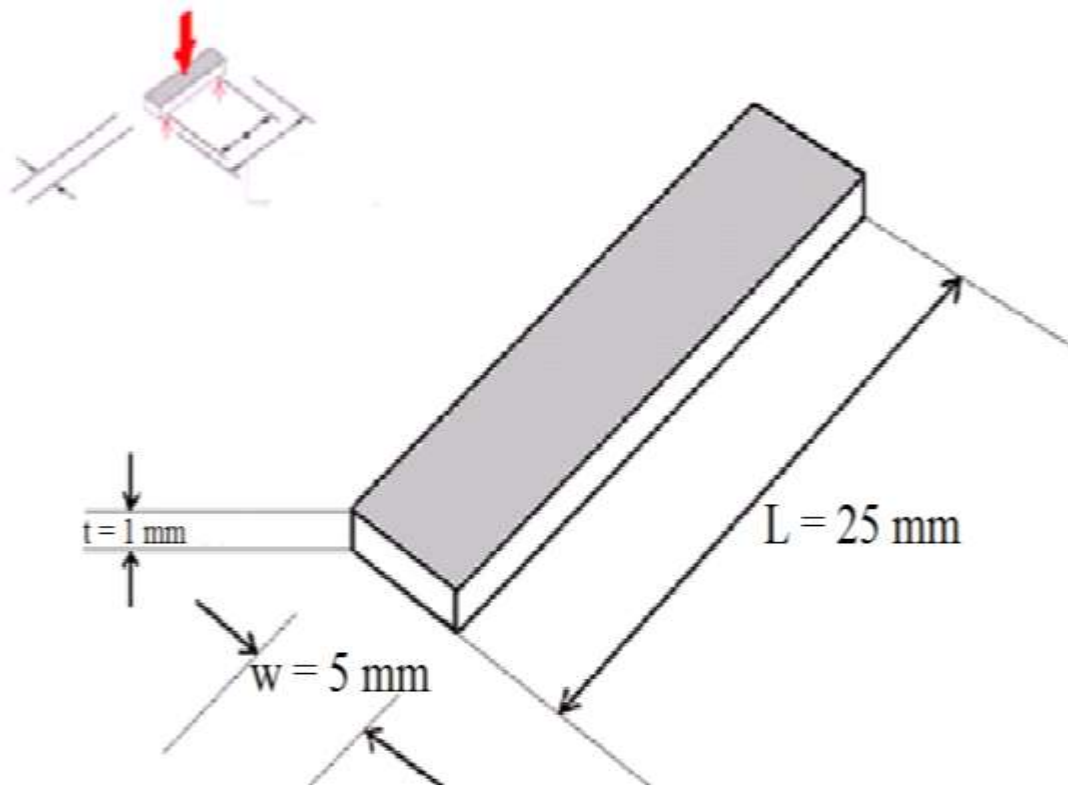


Figure 6. Sample dimensions (units: mm) for static mechanical tests: (A) ILSS, ASTM D 2344 (Liu and Nairn, 1990).

and after the crack forms

$$D = \frac{N_c + 1}{L} \tag{17}$$

It is proposed that fatigue data be analyzed using a modified Paris-law approach in which the rate of change in microcrack density is given by Equation 15, where A and n are two power-law fitting parameters. The conventional Paris-law approach relates the rate of change in crack length to the range in the applied stress intensity factor- ΔK . In the microcracking fracture experiment, the stress intensity factor approach is not possible and therefore ΔG is substituted for ΔK (Liu and Nairn, 1990).

In this research, the sample did not withstand longitudinal tensile

stress, hence σ_0 is equal to zero. As a result, Equation 13 changes into Equation 18.

$$G_m = \left(-\frac{\Delta\alpha(T_s - T_0)}{C_1} \right)^2 C_3 t_1 Y(D) \tag{18}$$

By substituting the necessary numerical values achieved by this experiment in Equation 18, G_m numerical value (energy release rate) is obtained. It appears from Equation 18 that as subtraction between T_0 and T_s increases, the numerical value of G_m increases. As mentioned before, $T_0 = 23^\circ\text{C}$; therefore, if the numerical value of $T_s = -175^\circ\text{C}$, the numerical value of G_m can be maximum.

For measuring the distance between the cracks, $2a$, such that the

Table 4. Void volume property results of UCFEC (M40J) as a function of vacuum thermal cycling: $E(x) \pm V(x)$ (Park et al., 2012).

V_{void} , (%)	1.50 ± 0.25	1.63 ± 0.31	1.66 ± 0.42	1.92 ± 0.51	2.28 ± 0.84
Cycles	0	500	1000	1500	2000

Table 5. Numerical values that are obtained from the equations in order to achieve an equation to express the crack density growth rate as a function of energy release rate.

C_w (m)	Cycle (n)	V_{void} (%)	N_c (-)	a (m)	ρ (-)
5e-5	0	1.5	8	1.8e-3	10.7
5e-5	1000	1.66	9	1.6e-3	9.4
5e-5	2000	2.28	12	1.1e-3	6.8118
5e-5	3000	3.72	19	7e-4	4.1667
5e-5	4000	5.62	29	4e-4	2.6786

width of each crack is assumed 5e-5 m, Table 4 (Park et al., 2012) is used. In the present research, the volume percent of void (V_{void}) in sample is assumed to be equal to longitudinal percent of void.

By using the numerical values in Table 4 and present assumptions, the numerical values in Table 5 are achieved. The numbers of cracks, N_c , are obtained from Equation 19 such that V_{void} is the void volume percent of sample, $L = 25$ mm, the sample length, and C_w is the crack width. It is important to notice that the LEO simulation experiment is performed for 2000 vacuum thermal cycles, and the approach used to obtain the void volume percent in sample for 3000 and 4000 cycles is explained in the following.

$$N_c = \frac{V_{\text{void}} * L}{C_w}, \quad (19)$$

In Table 4, the void volume percent in (M40J) UCFEC for the cycles 0, 500, 1000, 1500 and 2000 in LEO simulation experiment are shown. By using these data from Table 4, an equation to obtain the void volume percent in LEO simulation experiment in any cycle is possible. This equation indicates the void volume percent in UCFEC as a function of cycle numbers. By using this equation, and by applying partial derivative, obtaining the numerical value of void volume percent growth rate is possible. In this research, the void volume percent growth rate is assumed to be equal to crack density growth rate because it seems that the only void volume growth rate is due to crack density growth rate. It is noticeably the function of crack density growth rate obtained in this study (Equation 26) that indicates approximately the maximum of possible crack density growth rate.

$$V_{\text{void}} = aN^2 + bN + c. \quad (20)$$

At the beginning of the simulation experiment (0 cycles), the void volume percent is equal to 0.015, thus

$$0.015 = a(0)^2 + b(0) + c, \quad (21)$$

and at 1000 cycle, void volume percent is equal to 0.0166, therefore

$$0.0166 = a(1000)^2 + b(1000) + c, \quad (22)$$

In addition, at 2000 cycles, the void volume percent in sample is, 0.0228. As a result

$$0.0228 = a(2000)^2 + b(2000) + c. \quad (23)$$

Thus, by solving the three Equations (21, 22 and 23) bearing three unknown quantities (a, b and c), Equation 24 is obtained that indicates the void volume percent in sample as a function of the cycle numbers.

$$V_{\text{void}} = (2.9e - 9)N^2 - (1.3e - 6)N + 0.015. \quad (24)$$

$$\frac{dV_{\text{void}}}{dN} = (5.8e - 9)N - 1.3e - 6, \quad (25)$$

$$\frac{dV_{\text{void}}}{dN} = \frac{dD}{dN} = (5.8e - 9)N - 1.3e - 6. \quad (26)$$

In Figure 7, void volume as a function of cycle numbers in UCFEC in LEO simulation experiment is shown.

By applying the Equation 24 and substituting 3000 and 4000 as the number of cycles, the numerical values 0.0372 and 0.0562 for void volume percent are obtained. By employing partial derivative for Equation 24, void volume percent growth rate or crack density growth rate in LEO environment simulation experiment for UCFEC is obtained and indicated in Equations 25 and 26.

In Figure 8 (Park et al., 2012), the cumulative degradation of sample due to vacuum thermal cycles in LEO environment simulation experiment is shown.

Obviously, regarding Table 6 crack density numerical values of 0.3 to 0.3125 mm^{-1} , ΔG is increased; hence, the calibration of microcrack propagation is simple. Crack density as a function of cycle numbers is induced for different $\Delta \epsilon$ numerical values due to temperature change. In crack density numerical values of 0.3 to 0.3125 mm^{-1} , G_m is increasing (6.2172 to 8.7100 J/m^2). In this region, by obtaining the curve slope, the crack density growth rate and a relation between crack density growth rate and energy release rate are obtained. Subsequently, in this research, the results obtained from this relation are compared with the results from another fatigue life experiment for $[0_2/90_4]_s$ Fiberite 934/T300 composite under the mechanical cyclic load $\Delta \sigma_1 = 188.4$ MPa.

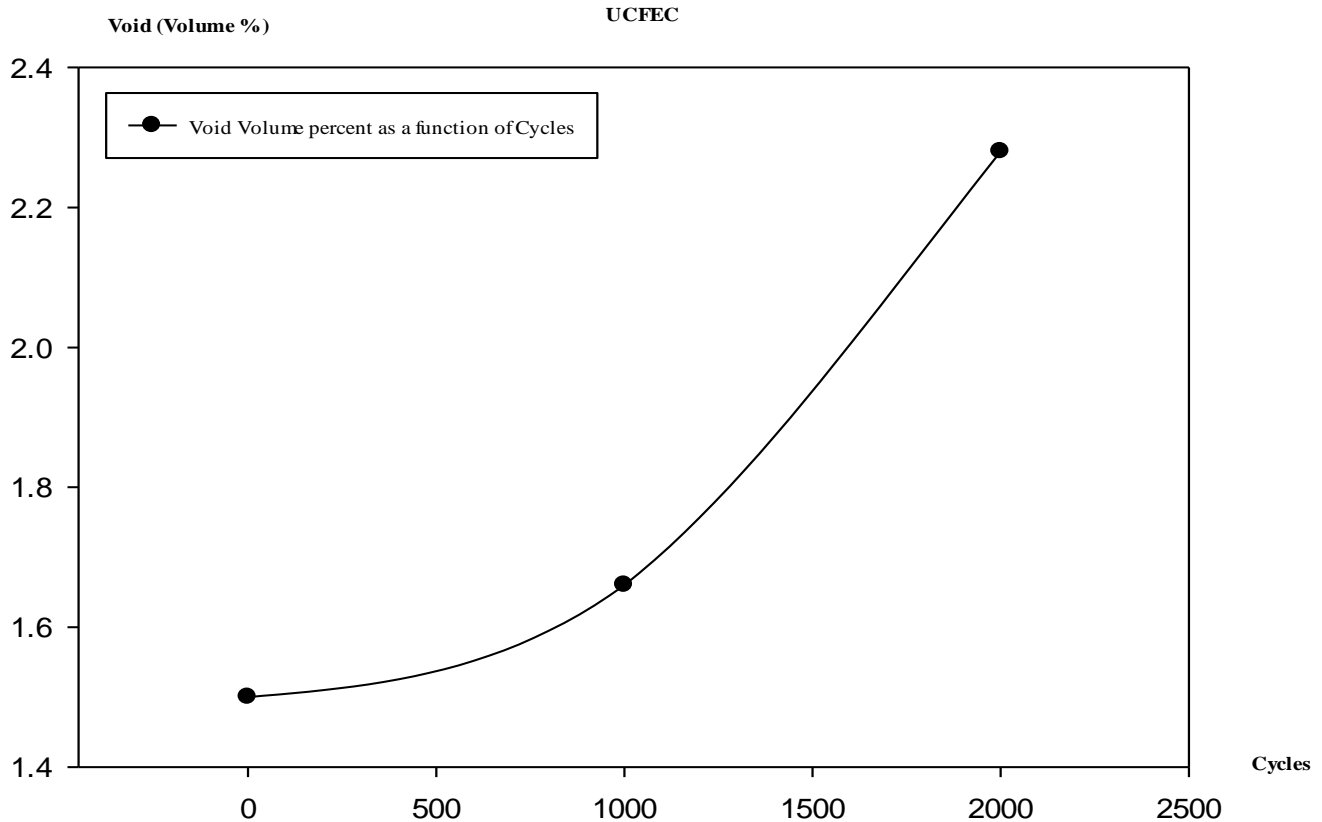


Figure 7. Void volume percent in sample as a function of cycle numbers in LEO simulation experiment.

Equation 27 is related to $[0_2/90_4]_s$ Fiberite 934/T300 composite under cyclic load, while Equation 28 is related to UCFEC in vacuum thermal cycles at LEO environment simulation experiment.

$$\frac{dC}{dN} = A\Delta G^{5.47}, \tag{27}$$

$$\frac{dD}{dN} = (5.897e-9)\Delta G^{3.0665}, \tag{28}$$

CONVEX CURVES METHOD

In this part of the study, a method for fatigue life prediction of UCFEC in LEO environment simulation experiment, by applying an analytical approach and using the experimental results, is achieved. The experimental results used to develop the convex curves method are obtained from vacuum thermal cyclic exposures (Park et al., 2012). In this method, by considering the data from experimental results and finding the points that develop convex curves, numbers of functions to predict the fatigue life of UCFEC are obtained.

Figure 9 (Park et al., 2012) indicates the results of LEO environment simulation experiment after going through 0, 500, 1000, 1500, and 2000 of vacuum thermal cycles. The functions obtained from these results are useful in predicting the fatigue life of UCFEC in satellite or space application, since UCFEC can be used in the structures of satellites and space crafts. In Figure 9, there are

many data for inter laminar shear strength (ILSS), flexural strength (FS), flexural modulus (FM), etc. In order to use the convex curves approach, for example in ILSS, Figure for M40J, using the three points (Cycles = 0, ILSS = 80.9), (Cycles = 1500, ILSS = 75.7), and (Cycles = 2000, ILSS = 69.1), and by solving three equations, three unknown quantities, like the method used to develop Equation 24, a convex curve is developed. This convex curve in a determined coordinate can intersect the cycle axis at zero ILSS. It means that, the numerical value of the cycle number achieved by this method can indicate the fatigue life of the UCFEC in LEO environment. This process to find more convex curves to predict the fatigue life is repeated. For the material M40J which is a UCFEC, only three convex curves: ILSS, flexural strength (FS), and flexural modulus (FM), from the data of the Figure 9 (Park et al., 2012) is obtained. The other data for M40J, such as longitudinal tensile strength, longitudinal compressive strength, longitudinal tensile modulus, and longitudinal compressive modulus can develop concave curves which might never intersect the cycle axis. Therefore, it seems, predicting the cycle number to failure by employing the concave curves is impossible.

The functions of convex curves obtained by this analytical method are indicated and shown in Table 7 and Figures 10 to 12, respectively. By solving Equation 29 while it equals to zero, a cycle number to FM failure is obtained; by solving the Equation 30 while it is equal to zero, a cycle number to ILSS failure is achieved; and by solving the Equation 31 while it equals to zero, a cycle number to FS failure is obtained. The cycle numbers for each failure are indicated in Table 8. It appears that the most likely fracture state is that of ILSS because the cycle number to failure for this state is the minimum cycle number.

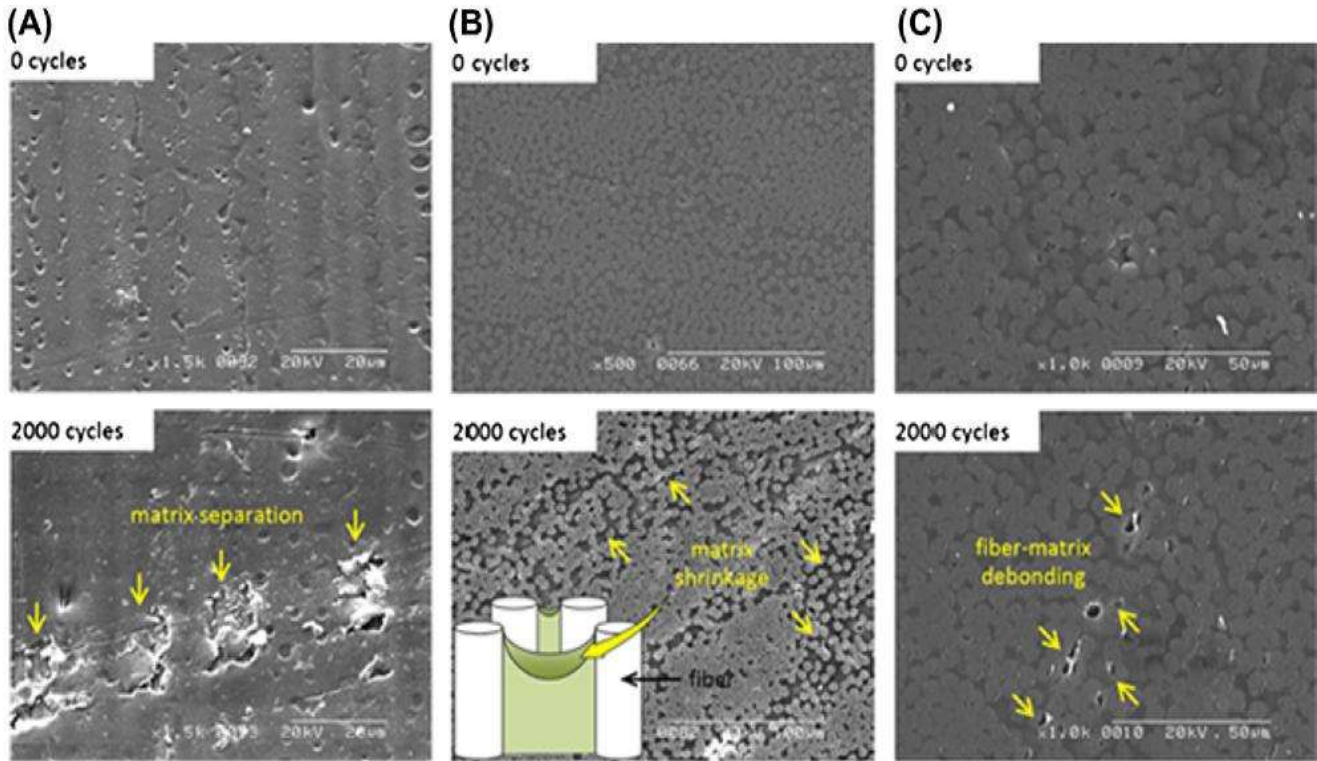


Figure 8. Electron micrographs showing different types of damage before and after vacuum thermal cycling: (A) laminate surface at 1500 x magnification showing matrix separation; (B) cross-sectional view at 500 x magnification showing matrix shrinkage; and (C) cross-sectional view at 1000 x magnification showing fiber-epoxy matrix debonding (Park et al., 2012).

Table 6. The numerical values that are obtained from the equations to achieve an equation of crack density growth rate as a function of energy release rate in LEO simulation experiment.

Cycle (n)	$Y(D)$ (-)	$G_{m, \text{Max}}$ at -175°C (J/m^2)	D (mm^{-1})
0	0.6802	6.2172	0.3000
1000	0.9529	8.7100	0.3125
2000	0.6330	5.7858	0.4400
3000	0.4677	4.2744	0.7194
4000	0.2614	2.3889	1.1201

Convex curves method analysis

Obviously, from Table 8, the minimum cycle numbers of fatigue life is due to ILSS. It means that, the cause of failure in UCFEC can be due to degradation in ILSS. In order to investigate the fracture process, it is reasonable to conclude that, as it seems that the result of degradation in ILSS is the main cause of fracture, it appears that the matrix debonding of UCFEC is the main cause of fracture. Thus, based on the convex curves method analysis, debonding between carbon fibers and epoxy is the most likely state of fracture. Therefore, it appears it is right to conclude that, because the number of cycle to failure obtained due to degradation of flexural modulus is greater than the number of cycle to failure due to degradation of ILSS, as a result, it is a second probable mode of fracture. Furthermore, it is concluded that, third probable state of fracture is due to the flexural strength degradation of UCFEC

because the cycle number to failure for this state is greater than the cycle number to failure due to degradation of flexural modulus. In Figures 13 and 14, the fracture phenomenon due to the degradation of UCFEC's ILSS exposed to vacuum thermal cycles is shown.

Fracture process analysis

As proven previously, it seems that the most likely state of fracture in UCFEC in LEO simulation experiment is the fracture due to the degradation of ILSS. Vacuum thermal cyclic fatigue, which is a non-mechanical fatigue is the main cause of failure in LEO environment. Hence, to analyze the fracture process, a thermal analysis is necessary.

While the UCFEC is exposed to sun illumination in LEO,

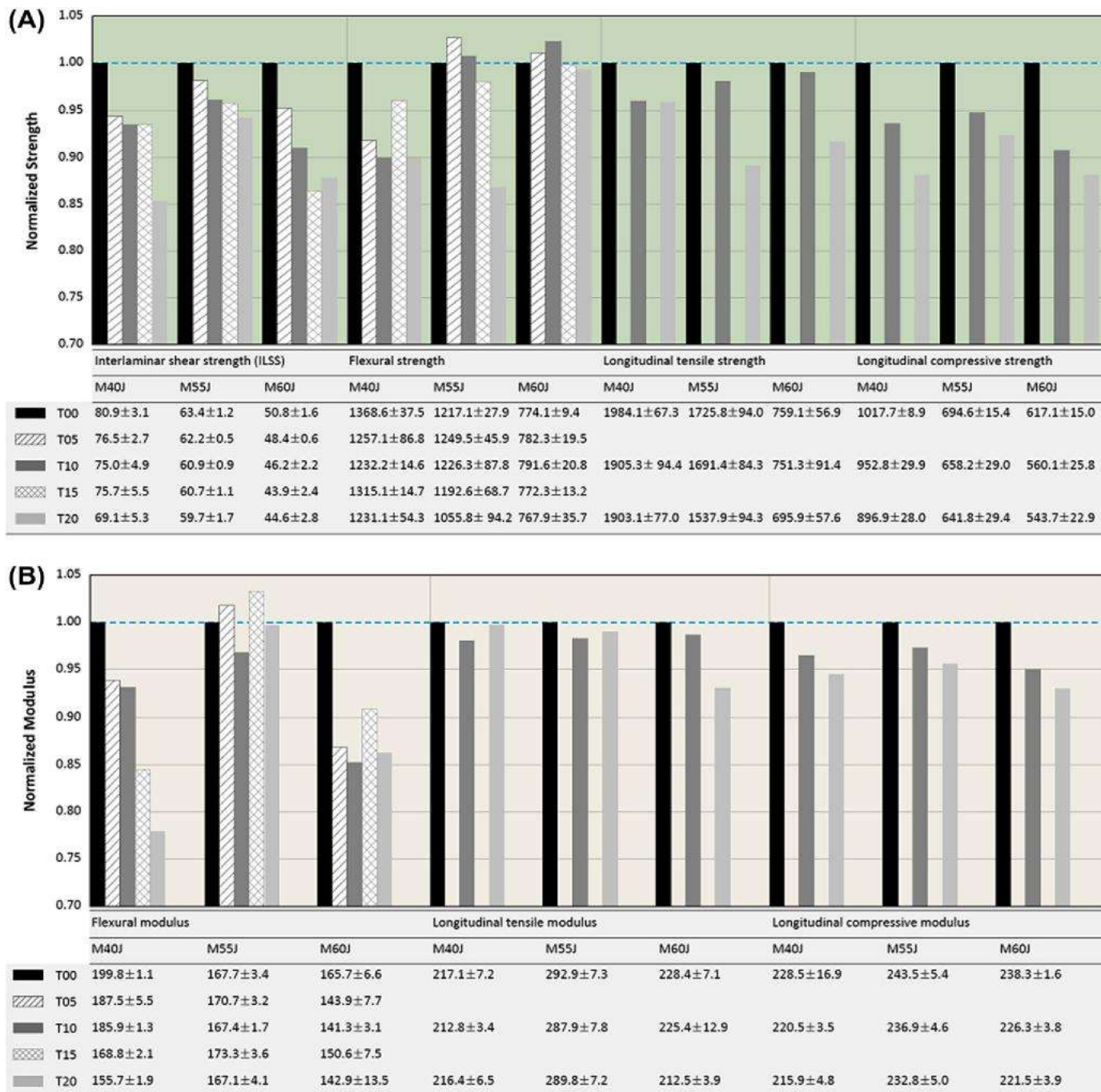


Figure 9. Mechanical property variations of the three kinds of unidirectional carbon fiber/epoxy laminate as a function of vacuum thermal cycling (mean value $E(x) \pm$ variation $V(x)$): (A) static strength variations; and (B) elastic modulus variations (Park et al., 2012).

temperature raises from 23 to 120°C. In UCFEC, due to longitudinal coefficient of thermal expansion for carbon fiber and epoxy which are negative and positive respectively, carbon fiber tends to contract in longitudinal axis; however, epoxy tends to expand in longitudinal axis. In this state, carbon fiber withstands tensile force while epoxy withstands compressive force. Whereas the UCFEC is exposed to solar eclipse in LEO, temperature decreases from 23 to -175°C. In this condition, the epoxy withstands tensile force while the carbon fiber withstands compressive force. Because the carbon fiber and epoxy are stuck together, due to this reverse behavior of

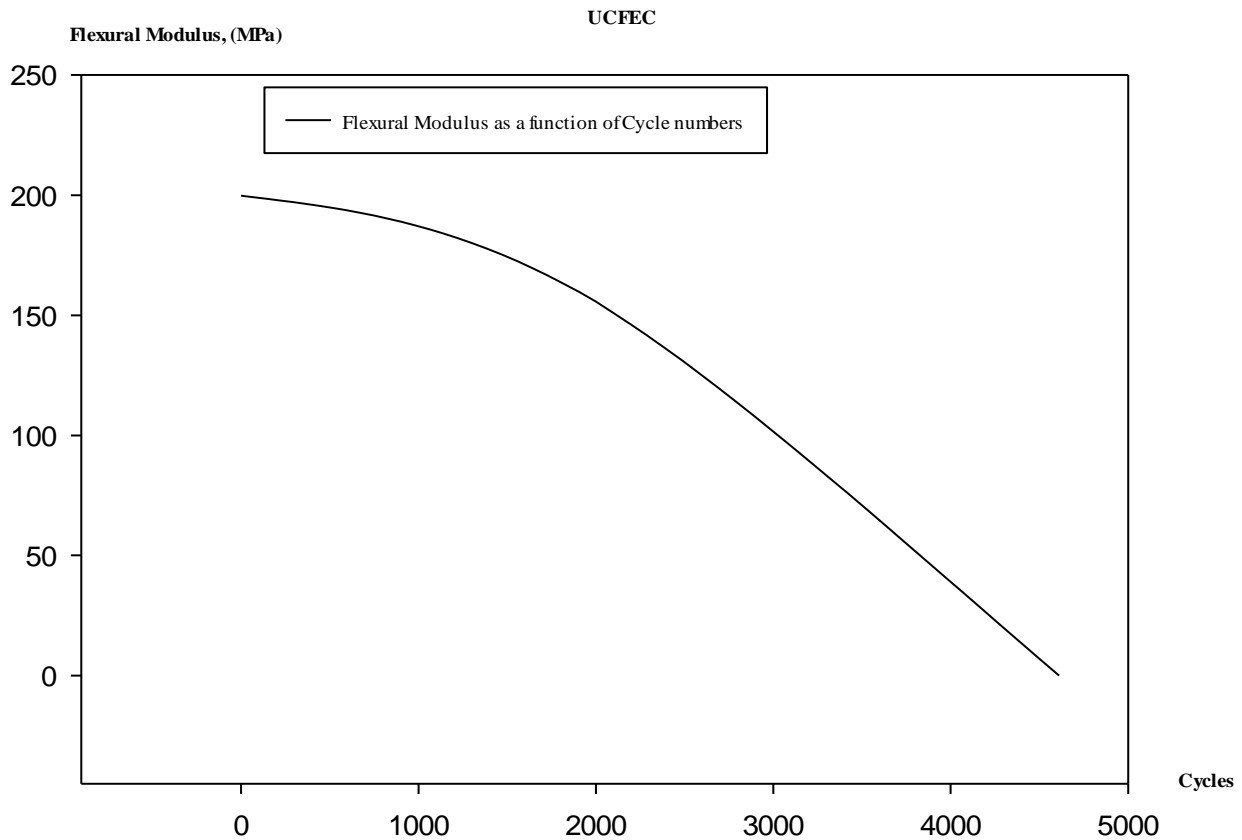
carbon fiber and epoxy in longitudinal direction, cracks are induced especially in the interface-bonding surface between fiber and matrix. By continuing the thermal cycles, the cracks are propagated and by the propagation of cracks, ultimately, the fracture is occurred.

STEADY-LINEAR METHOD

In this part of the study, a method to predict the fatigue life of

Table 7. Functions that are obtained from data in Figure 9 and Table 4.

Equation Name and Number	Functions
V_{void} (24)	$V_{\text{void}} = (2.9e - 9)N^2 - (1.3e - 6)N + 0.015$
FM, (MPa) (29)	$FM = (-8.15e - 6)N^2 - (5.75e - 3)N + 199.8$
ILSS, (MPa) (30)	$ILSS = (-4.87e - 6)N^2 + (3.84e - 3)N + 80.9$
FS, (MPa) (31)	$FS = (-6.617e - 5)N^2 + (6.358e - 2)N + 1368.6$

**Figure 10.** Flexural modulus as a function of cycle numbers created by data in Figure 8 (Cycles = 0, FM = 199.8), (Cycles = 1000, FM = 185.9), and (Cycles = 2000, FM = 155.7), in LEO environment simulation experiment.

UCFEC in Mars environment is proposed. In order to achieve this method, the results of convex curves method are employed. As proven by convex curves method, the main cause of fracture in UCFEC in low earth orbit exposed to vacuum thermal fatigue is due to the degradation of ILSS between carbon fiber and epoxy. Because the only non-mechanical cyclic load that exists in LEO and Mars environment is the thermal cyclic load, the results of convex curves method can be applied to predict the fatigue life on Mars.

Based on this assumption, temperature variation in Mars is the main thermal-fatigue load and cause of degradation in ILSS, FM, and increasing Void Volume in UCFEC.

One cycle in LEO was designed as the sequence from 120 to -175°C and back to 120°C (Park et al., 2012). On Mars, temperature varied each day and night between 35 and 50°C (Pasachoff, 1993).

According to these data, the temperature variation of satellite in LEO at each cycle around the earth is 295°C; however, maximum temperature variation in each night and day on Mars is 50°C (Pasachoff, 1993). Therefore, the temperature variation in LEO for the satellite circulating around the earth is 5.9 times of temperature variation on night and day in Mars for the aerospace structure that landed on Mars.

Steady-linear method to obtain ILSS of UCFEC on Mars

Based on Equation 35, for a specific carbon fiber/epoxy composite, the only factor that can have effect on the Inter laminar Shear stress (ILSSs) is the temperature variation. This assumption can be

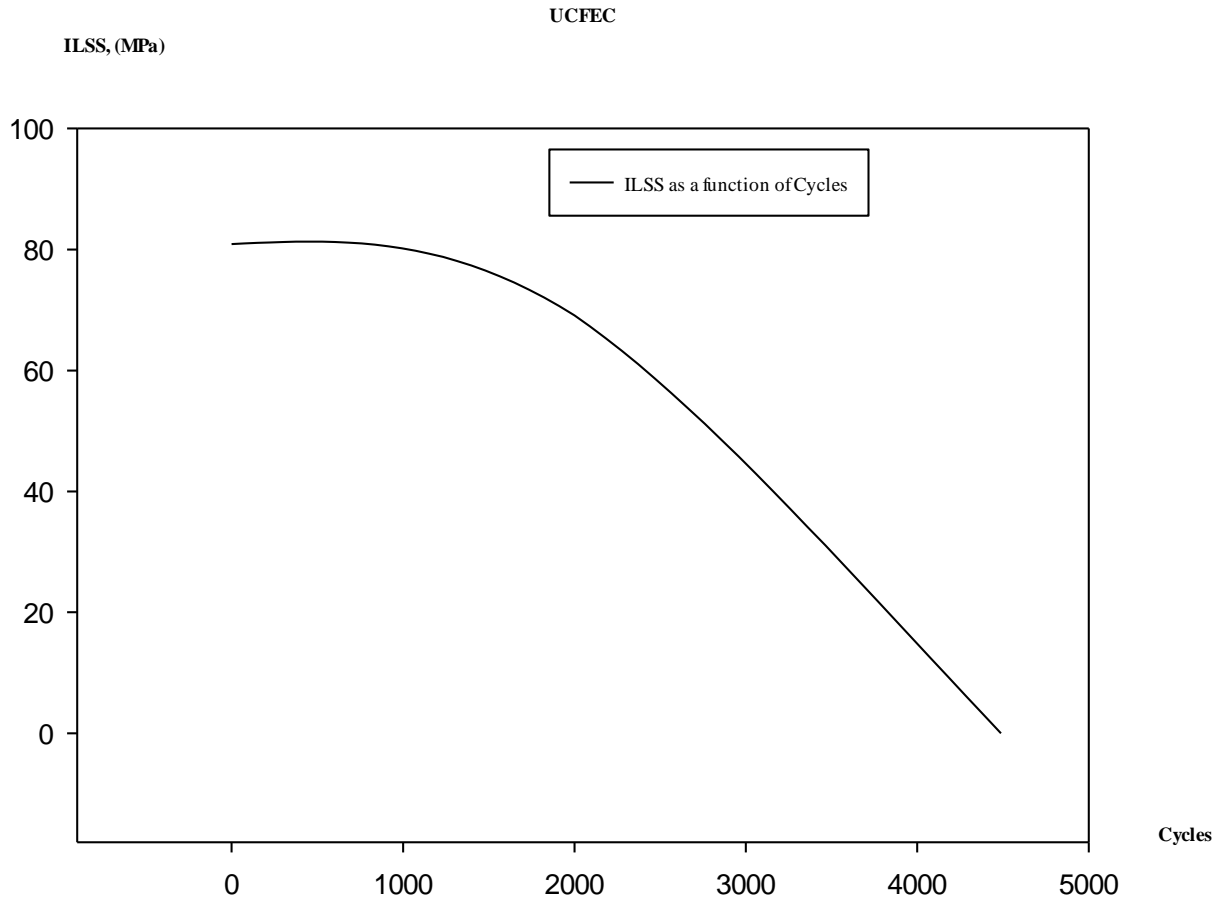


Figure 11. ILSS as a function of cycle numbers in LEO environment simulation experiment.

valid because it is assumed that other factors like coefficients of thermal expansion and shear modulus of UCFEC remain constant. Hence, by referring to ILSS equation achieved by convex curves method while it equals the relation (32), cycle numbers for the steady region of the steady-linear method can be obtained.

In the following equations, $ILSS_0$ of UCFEC is ILSS at zero cycle. Temperature variation on Mars, ΔT (on Mars) equals 50°C and in LEO equals 295°C . ILSS equation achieved by convex curves method is

$$ILSS = (-4.87e - 6)N^2 + (3.84e - 3)N + 80.9, \quad (30)$$

and the relation (32) can be defined as

$$\frac{ILSS_0 * \Delta T \text{ (on Mars)}}{\Delta T \text{ (in LEO)}}, \quad (32)$$

Inter laminar shear strength at zero cycle for UCFEC in LEO experimental simulation is 80.9 MPa (Anvari, 2014). Based on this approach, while ILSS equation is equal to the relation (32), the following relation is obtained.

$$(80.9*50)/(295) = (-4.87e - 6)N^2 + (3.84e - 3)N + 80.9. \quad (33)$$

By solving the relation (33), the cycle number, N , is equal to 4129.

With the result obtained followed by the presented procedure, it can be concluded that for the cycle numbers less than 4129, inter laminar shear strength remains constant. However, based on convex curves shapes, after the specific numerical values of cycle numbers, the numerical quantities of ILSS is decreased. This diminishing of ILSS in UCFEC due to thermal cycles can be approximated by a line with the negative slope. This approximated line can be observed in the convex curves figures between the 3000 to 4000 cycles (Figures 10 to 12).

In convex curves method, the decrease in ILSS is due to the LEO environmental condition. Here in this study, a method is required to transform these curves to s-shape that can be related to Mars environment. However, it is apparent that by decreasing the temperature variation cycle from 295 to 50°C in LEO (around the Earth) to Mars (day and night), the amplitude of thermal cycle stress decreases. By diminishing the amplitude of thermal cycle stress from LEO to Mars, it is expected that the fatigue life of UCFEC increases because the less the range of thermal cycle stress is, the more fatigue life exists. This tangible fact can explain that the convex curves need to be extended to indicate more fatigue life on Mars in comparison to LEO. This extension can be accomplished by stretching the convex curves in a state that they represent more fatigue life. Because the temperature variation on LEO is at least 5.9 times of that on Mars, it is proposed that if the ILSS equation achieved by the convex curves method is equal to $ILSS_0$ divided by 5.9, we might be able to illustrate how many thermal cycles on Mars ILSS is steady. But after the steady region, a new assumption is required. This theory states that, because of decreasing section of

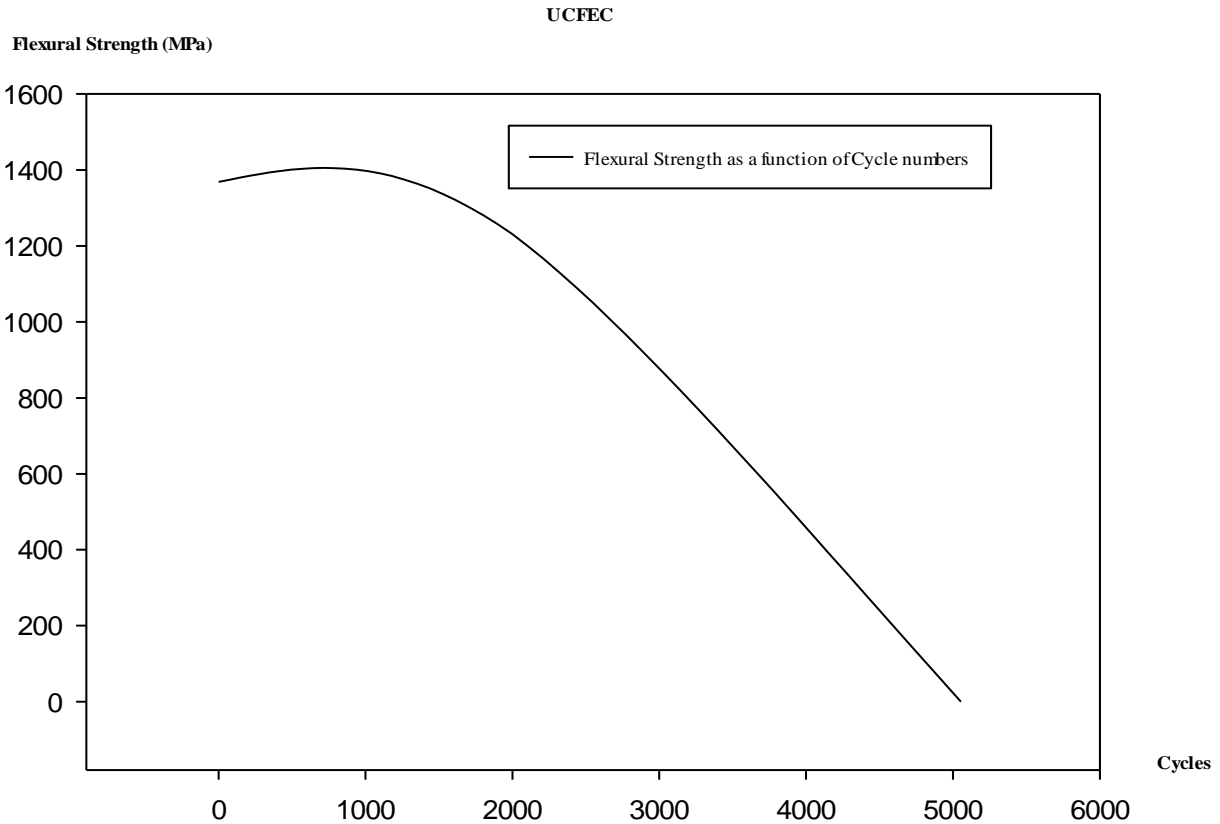


Figure 12. Flexural strength as a function of cycle numbers created by data in Figure 8 (Cycles = 0, FS = 1368.6), (Cycles = 1500, FS = 1315.1), and (Cycles = 2000, FS = 1231.1), in LEO environment simulation experiment.

Table 8. Number of fatigue life cycles for each function.

Equation name and number	Critical functions	Cycle no. to failure (N_f)
V_{void} (24)	$1 = (2.9e - 9)N^2 - (1.3e - 6)N + 0.015$	18655
FM, (MPa) (29)	$0 = (-8.15e - 6)N^2 - (5.75e - 3)N + 199.8$	4611
ILSS, (MPa) (30)	$0 = (-4.87e - 6)N^2 + (3.84e - 3)N + 80.9$	4488
FS, (MPa) (31)	$0 = (-6.617e - 5)N^2 + (6.358e - 2)N + 1368.6$	5053

convex curves figures, there is an approximated linear part with negative slope (between 3000 to 4000 cycles); this slope can be divided by 5.9 (Temperature variation in LEO to Mars each night and day) to indicate the linear part for the Mars environmental condition. After these procedures, the linear part can be attached to the end of steady part. This process can be employed to derive the equations and figures for the ILSS and FM on Mars. The following results are obtained by this procedure. Based on these assumptions, if temperature variation on Mars is equal to 50°C, then for cycles between 4129 and 19907, ILSS is equal to

$$(ILSS_{50}) = -5.12712e-3(N) + 102.0698785 \quad (34)$$

ILSS degradation is a function of Cycle numbers due to 50 Celsius temperature variation between day and night on Mars in UCFEC as

illustrated in Figure 15.

Steady-linear method to obtain FM of UCFEC on Mars

Obviously, because of reverse behavior between carbon fiber and epoxy due to their different coefficients of thermal expansion, there is always ILSs (inter laminar shear stress) between carbon fiber and epoxy. Thus, while the ILSS equation is equal to ILSs equation, the numerical value of fracture cycle number can be achieved. Furthermore, it is important to mention that the temperature variation in the following equation is the temperature difference from the sample's crack free temperature. Crack free temperature is the temperature that the sample is uncracked. In the presented research, this temperature is 23°C (Anvari, 2014).

Cooling

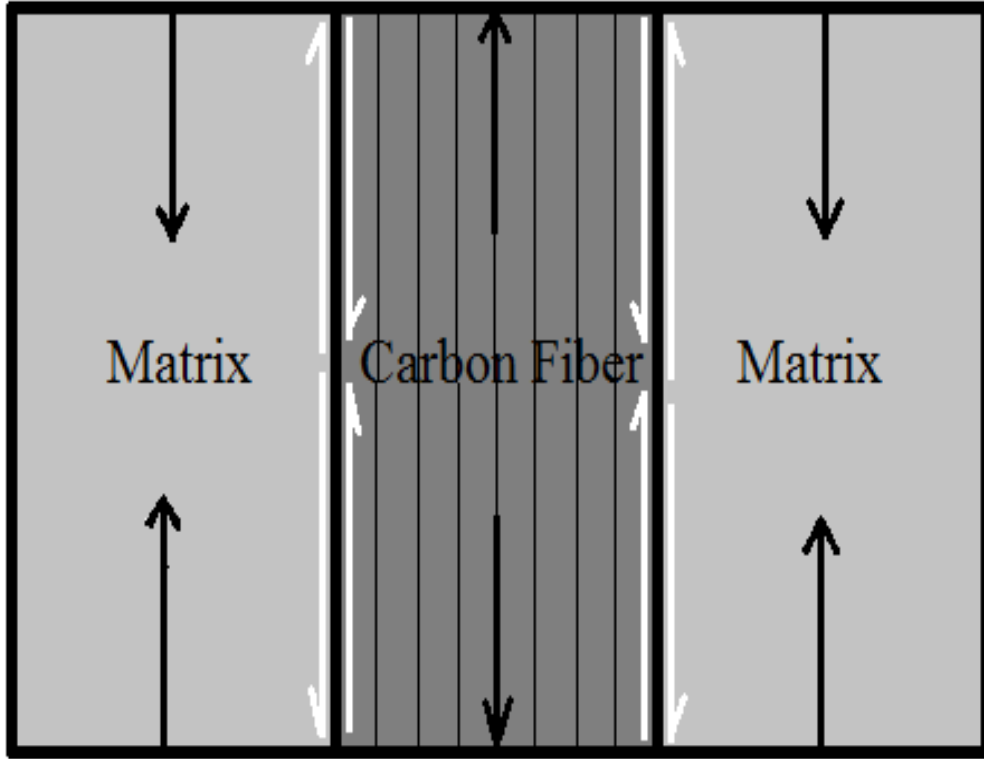


Figure 13. Edge view of UCFEC in simulation for solar eclipse in LEO environment simulation experiment. Black arrows show the expansions and contractions direction and white arrows show the compression or tension stress between the carbon fiber and matrix.

$$ILSs = \Delta\alpha\Delta T.G, \tag{35}$$

$$ILSs = (\alpha_c - \alpha_f)(T_0 - T_s)G, \tag{36}$$

$$ILSs = (\alpha_c - \alpha_f)(T_0 - T_s)(FM / 2(1 + \nu)), \tag{37}$$

In the indicated Equations 36 and 37 that are achieved by application of Equation 35 (Maheswari and Prasad, 2013), FM is the Flexural Modulus of UCFEC, G is the shear modulus of UCFEC, and GI is carbon fiber axial shear modulus.

$$G = (G_c + G_f) / 2, \tag{38}$$

$$\nu = (\nu_c + \nu_f) / 2. \tag{39}$$

In Equation 39, ν is the Poisson's ratio of UCFEC, ν_c is epoxy Poisson's ratio, and ν_f is carbon fiber axial Poisson's ratio. This is

important to notice that, by applying the steady-linear approach, the FM equation on Mars is derived and shown in Figure 16. In order to develop this figure, FM convex curve is employed. Based on the results of steady-linear method, if the temperature variation on Mars between day and night is 50°C and cycle numbers are less than 4173, as a result, FM is equal to 199.8 MPa. Furthermore, by applying steady-linear method, it is obtained that, for cycle numbers between 4173 and 22951, the FM equation is

$$FM = -1.064e-2(N) + 244.20072 \tag{40}$$

The above equation is obtained with the same method to derive the steady-linear equation for ILSS on Mars, but the only difference is that instead of using $ILSS_0$, FM_0 and instead of applying ILSS convex curve, FM convex curve is used.

Steady-linear method to obtain void volume in UCFEC on Mars

In order to obtain equations to estimate the void volume in UCFEC on Mars, it is assumed that before the numerical value of $N_{steady} = 4129$, that is, the N_{steady} in ILSS equations for Mars environment, the void volume remains constant (void volume at zero cycle (V_{void0}))

Heating

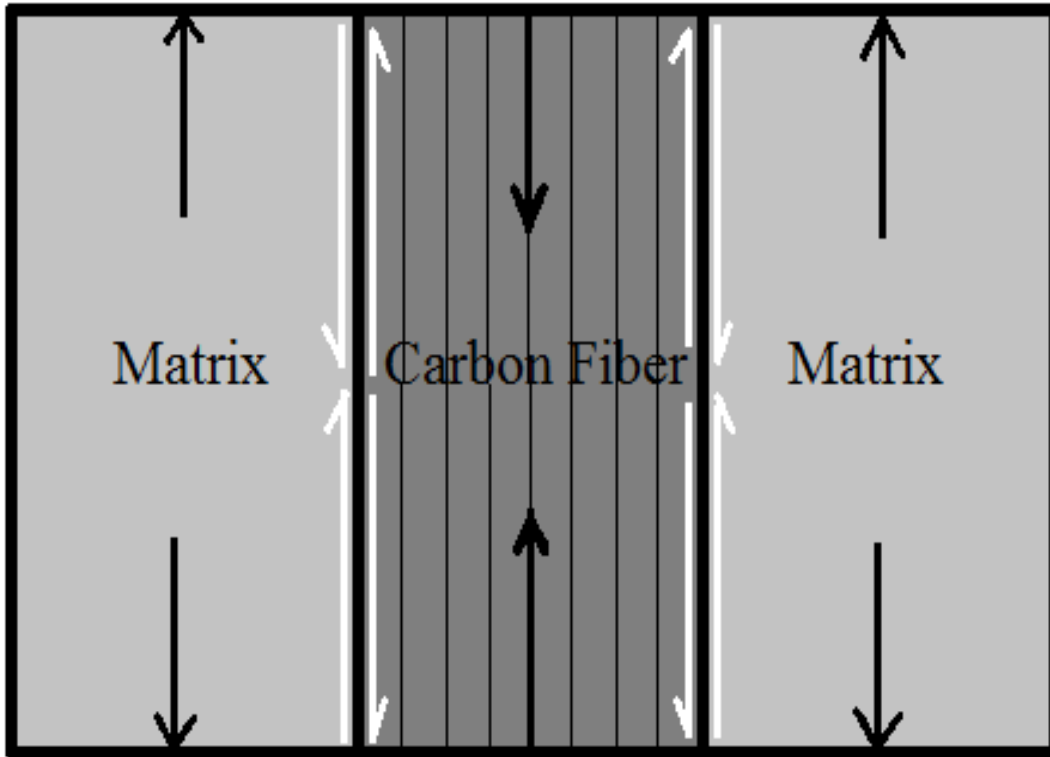


Figure 14. Edge view of UCFEC in simulation for sun illumination in LEO environment simulation experiment. Black arrows show the expansions and contractions direction and white arrows show the compression or tension stress between the carbon fiber and matrix.

= 0.015). This assumption is based on the fact that because the ILSS in steady-linear method remains constant in these regions, the material properties and characteristics remain constant. Therefore, void volume remains the same numerical value ($V_{void0} = 0.015$). For the greater numerical quantities of N_{steady} , by solving void volume equation (Equation 24) while it equals the relation (41), the numerical value for the fracture cycle on Mars, based on the void volume in UCFEC, can be obtained. The final cycle number to fracture on Mars (N_f), according to the void volume is 45224.

$$\frac{1 * \Delta T(\text{in LEO})}{\Delta T(\text{on Mars})}, \tag{41}$$

$$V_{void} = (2.9e - 9)N^2 - (1.3e - 6)N + 0.015. \tag{42}$$

With the results available following the mentioned procedure, it is convenient to develop the steady-linear figure for the void volume as a function of cycle numbers. For the cycle number values less than 4129, the void volume in UCFEC remains constant (0.015) and for the greater cycle numerical quantities, the void volume

increases to finally reach the maximum amount at 45224 cycle numbers. In figure 17, this process is observable. In order to develop the linear region equation in the following figure, two boundary conditions that represent two points, are as follow: $N = 4129, V_{void} = 0.015$ and $N = 45224, V_{void} = 1$. These two points are employed to create a relation, with two equations, two unknown quantities method. By following this method, there are

$$V_{void} = gN + h, \tag{43}$$

$$0.015 = g(4129) + h, \tag{44}$$

$$1 = g(45224) + h, \tag{45}$$

as a result of the above procedure, for the cycle numbers less than 4129, void volume is equal to 0.015, and if the cycle numbers are between 4129 and 45224, void volume equation is

$$V_{void} = 2.397e-5(N) - 0.083967 \tag{46}$$

In the linear region, $4129 < N \leq 45224$, void volume growth rate that

ILSS Degradation of UCFEC

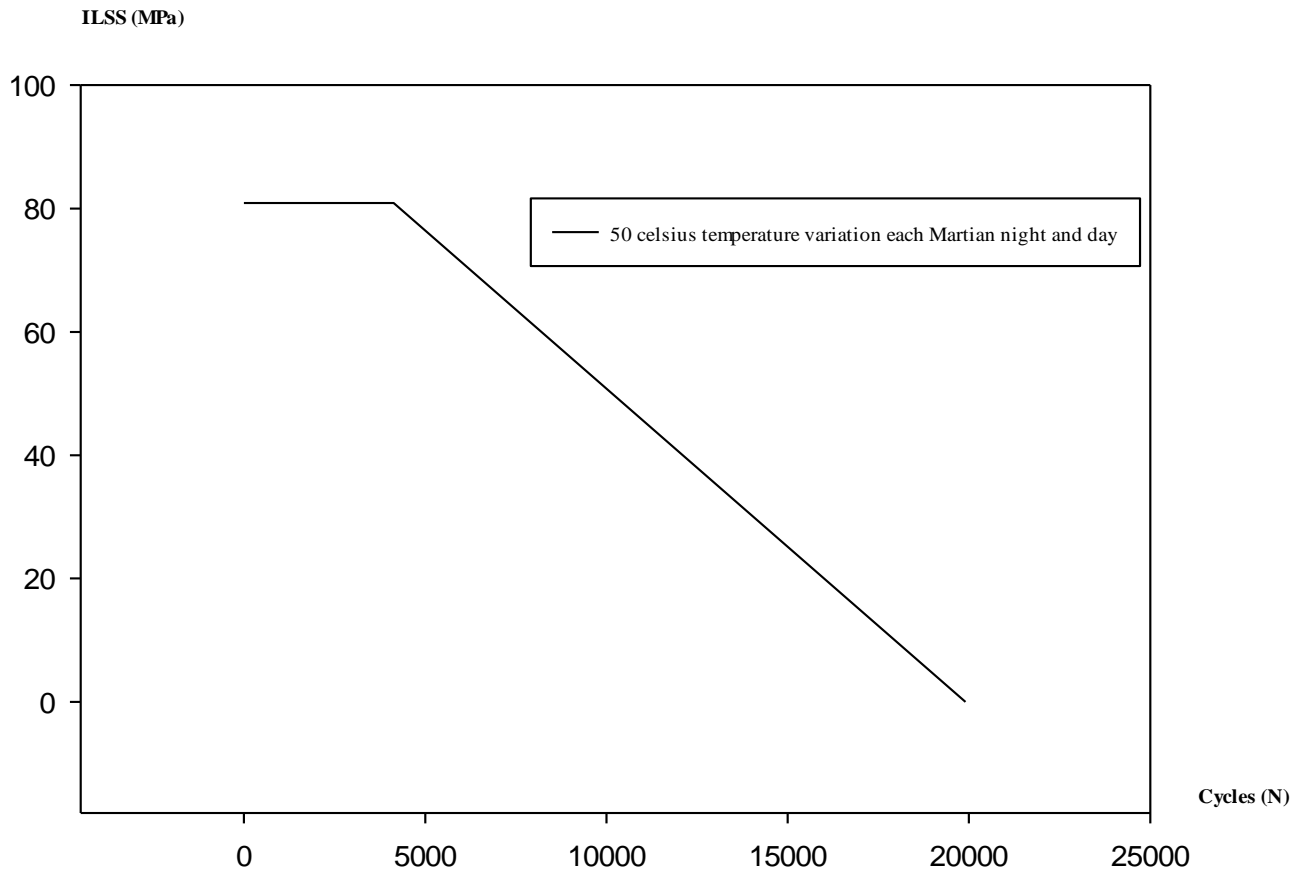


Figure 15. ILSS degradation as a function of cycle numbers in 50°C temperature variation between day and night on Mars.

in this study is assumed to be equal to crack density growth rate is defined as

$$(dV_{void}/dN) = (dD/dN) = 2.397e-5 \tag{47}$$

In Figure 17, void volume as a function of cycles in UCFEC for 50°C temperature variation each night and day on Mars is illustrated.

Applying steady-linear method

By applying Equation 48, the fatigue life of UCFEC on different seasons on Mars in night and day can be approximated. As previously obtained in this study, at 50°C temperature variation between night and day on Mars for cycle numbers 4129 to 19907, inter laminar shear strength function is:

$$ILSS = -5.12712e-3(N) + 102.0698785$$

Furthermore, as previously calculated in this study, for cycles 4173 to 22951, the flexural modulus equation is as follows:

$$FM = -1.064e-2(N) + 244.20072$$

$$ILSS = -(\alpha_c - \alpha_l)(T_0 - T_s)(FM / 2(1 + \nu)) \tag{48}$$

In order to obtain the fatigue life at coldest winter night on Mars with the application of Equation 48, the following data are required. $T_0 = 150K (-123°C)$ at winter night on Mars (Pasachoff, 1993), the numerical values of α_c and α_l are indicated in Table 1, $T_s = 23°C$ (crack free temperature) (Park et al., 2012), ν is the Poisson's ratio of UCFEC obtained by Equation 39, G is the shear modulus of UCFEC obtained by Equation 38; and substituting Equations 34 and 40 into Equation 48, for ΔT (on Mars) = $(T_{Day} - T_{Night}) = 50°C$, Equation 48 can be changed into a new relation. By solving the mentioned relation, N is equal to 19891 cycles, that is, the fatigue life of UCFEC on coldest winter night on Mars. It is important to notice that the numerical value of $(T_0 - T_s)$ in the relation is the maximum numerical value. Consequently, the Inter laminar shear stress is the maximum numerical amount, decreasing the fatigue life from 19907 cycles at zero ILSSs to 19891 cycles at maximum ILSSs. By employing Equation 48, this procedure can be repeated for all the temperatures on Mars in day and night in different seasons. With this method, by applying Equation 48, the fatigue life of UCFEC on Mars in all the temperatures can be evaluated.

FRACTURE IN UCFEC ON MARS DUE TO THERMAL FATIGUE

As proven previously, and based on Equation 48, since the temperature difference from 23°C (crack free temperature) is increased, the ILSSs between carbon fiber and epoxy is increased. The temperature variation on Mars is from 150K (-123°C) to over

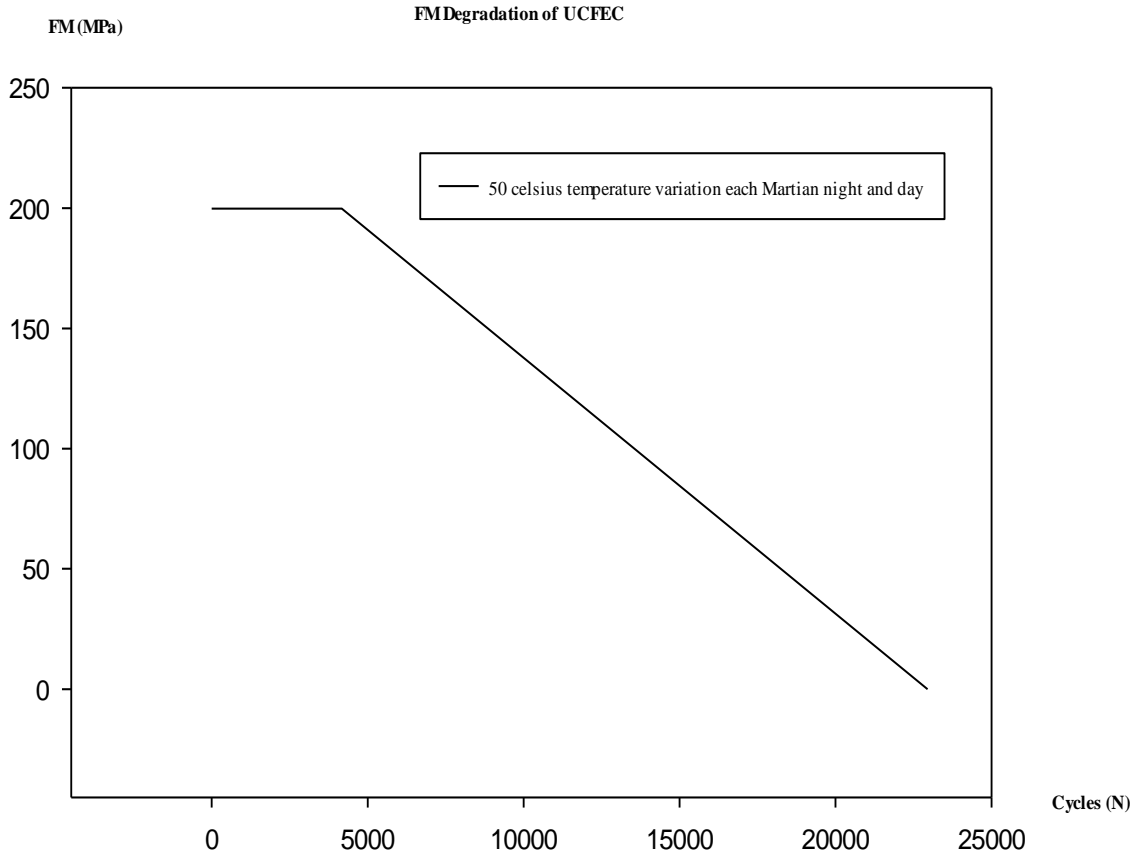


Figure 16. FM degradation as a function of cycle numbers in 50°C temperature variation between day and night on Mars.

300K (27°C) (Pasachoff, 1993). Consequently, based on this knowledge, it appears that the temperature variations in winter is almost from 150K at winter night because of solar eclipse, to about 200K in winter day because of sun illumination in day. In autumn and spring, it is from almost 200K at night to about 250K in day. Additionally, in summer, temperature is from almost 250K at night to about 300K (27°C) in day.

Based on these approximated conclusions, it is easy to estimate the probability of fracture for UCFEC on Mars night in comparison with Mars day in different seasons. By using relation (49), this estimation is possible. As concluded in Table 9, the probability of fracture at summer night is almost 11.5 times of summer days on Mars which is the maximum. The probability of fracture at coldest winter night is about 1.52 times of winter days, which is the minimum. This fact is concluded because the temperature at night is lower than the temperature in day and the maximum temperature at night on Mars is almost 250K. This implies that the variation of temperature from standard temperature in UCFEC (23°C) at nights is always greater than the variation of temperature in days. Thus, as the difference between the environmental temperature in Mars and UCFEC crack free temperature is increased, inter laminar shear stress is increased. Increase of inter laminar shear stress can be the cause of fracture in UCFEC because it can attain inter laminar shear strength of UCFEC. As proven by convex curves method, the main cause of fracture in UCFEC exposed to vacuum thermal cycles is due to degradation of inter laminar shear strength.

In relation (49), it can be concluded that for UCFEC, all the factors are related to material properties except the temperature

variation from the standard temperature ($T_s = 23^\circ\text{C}$). Consequently, the only factor that can affect the ILSs is the temperature variation because the temperature difference from the UCFEC uncrack temperature is the main cause in inducing inter laminar shear stress. Hence, it can be the main cause of fracture in UCFEC as proven by convex curves method.

$$\frac{ILSs1}{ILSs2} = \frac{(\alpha_c - \alpha_l)(T_{\text{Night}} - T_s)G}{(\alpha_c - \alpha_l)(T_{\text{Day}} - T_s)G}, \quad (49)$$

$$\frac{ILSs1}{ILSs2} = \frac{(T_{\text{Night}} - T_s)}{(T_{\text{Day}} - T_s)}, \quad (50)$$

fracture at nights (FN) can occur FN times in comparison with fracture in days in specific season.

$$FN = \Delta T_{\text{Night}} / \Delta T_{\text{Day}}, \quad (51)$$

$$FN = \frac{(T_{\text{Night}} - T_s)}{(T_{\text{Day}} - T_s)}. \quad (52)$$

In the Table 9, by applying mentioned relations, probabilities of fracture in UCFEC in Mars nights in comparison with Mars days in different seasons are indicated.

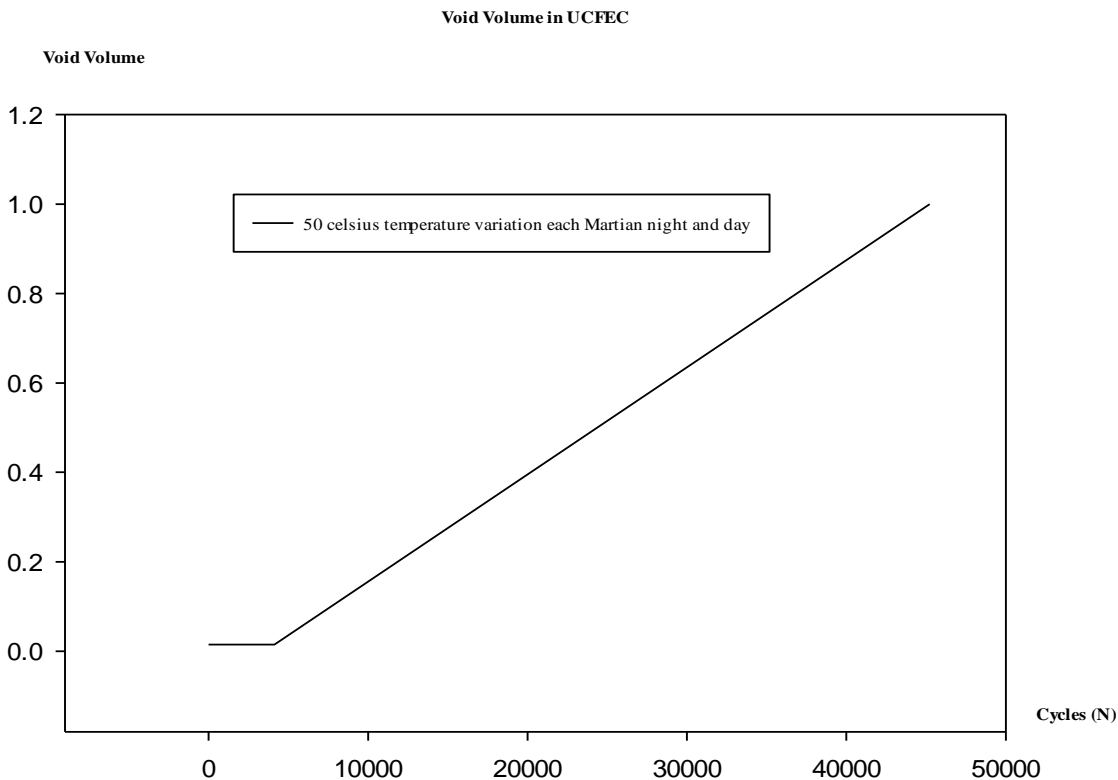


Figure 17. Void volume in UCFEC as a function of cycle numbers at 50°C temperature variation between day and night on Mars.

Table 9. Probability of fracture in UCFEC at night in comparison with day at 50°C temperature variation between night and day in different seasons on Mars.

Winter	Autumn and Spring	Summer
1.52	2.09	11.5

CARBON FIBER’S PARALLEL CRACK PROPAGATION METHOD

Multiple matrix cracks, also called intra laminar cracks, are observable in layer with off-axis orientation with respect to the main loading direction. These cracks are usually initiated in weakest positions or in stress concentration areas, as they cover the whole layer thickness and grow parallel to fibers in the layer (Giannadakis and Varna, 2009). During each loading cycle where the damage growth threshold is exceeded, the fiber/matrix interface crack will grow parallel to the fiber for a length da according to the crack growth law (Uleck, 2006).

In this method, by using experimental data (Nakamura et al., 2007), the crack growth rate in Mars environment (50 Celsius temperature variation between day and night on Mars) is obtained and by applying the relation (55), the cycle numbers to fracture of UCFEC on Mars is approximately achieved.

Experimental procedures

To determine properties of present composite lamina, separate 8-ply specimens with unidirectional fiber were fabricated using the

same vacuum bagging process. The thermal cycle tests were conducted using the environmental chamber. In the current experiments, in order to isolate the effects of thermal cycles, the rh was set at 0%. Total of five different amplitudes of $\Delta T = 140, 60, 30, 100, 120^\circ\text{C}$ were prescribed during the measurement period. At initial phase, it took about 240 cycles to reach steady state propagation under $\Delta T = 140^\circ\text{C}$ condition. During the steady state, the growth rate was estimated to be $da/dN = 5.1 \mu\text{m/cycle}$. At 500th cycle, the temperature amplitude was switched to 60°C and maintained for 100 cycles. The smaller number of cycles were chosen since it appeared that the propagation have reached the steady state much faster but at slower rate of about $da/dN = 1.7 \mu\text{m/cycle}$. In the subsequent phase (after 600 cycles), ΔT was reduced to 30°C . Even after 80 cycles, the measurements showed no visible change in the crack length (Nakamura et al., 2007).

Problem formulation

In Equation 53, $L = 25 \text{ mm}$ is the length of UCFEC sample, that is the length of carbon fiber as well. L_{void} is the void length in UCFEC sample that is equal to the length of sample multiplied by void volume defined in the following relation.

Table 10. Numerical values obtained by the equations in “Problem Formulation” to achieve crack density growth rate as a function of energy release rate in 50°C temperature variation each Martian night and day at coldest Martian nights in winter (-123°C).

Cycle (n)	Y(D) (-)	G _{m, Max, at -123°C (J/m²)}	D (mm ⁻¹)
4129	0.6802	5.0594	0.3000
4195	0.9529	7.0878	0.3125
4454	0.6330	4.7084	0.4400
5054	0.4677	3.4788	0.7194
5847	0.2614	1.9443	1.1201

Table 11. Fatigue life of UCFEC in different environment conditions on Mars.

Fatigue Life of UCFEC on Mars	Cycle number to fracture	Martian time to Fracture (one Martian year is equal to 23 earth’s months)
Steady-Linear Method, Mars Summer day at 27°C, T _{Day} -T _{Night} =50°C	19907	28 years, 19 months, and 16 days
Steady-Linear Method, Mars Winter night at -123°C, T _{Day} -T _{Night} =50°C	19891	28 years, 19 months, and 0 day
Carbon fiber’s parallel crack propagation method for T _{Day} -T _{Night} =50°C	≤ 21734	≤ 31 years, 11 months, and 13 days
Difference between steady-linear method at Mars Summer day with T _{Day} -T _{Night} =50°C and carbon fiber’s parallel crack propagation method for T _{Day} -T _{Night} =50°C (at N ≤ 21734)	≤ 1827 ≤ (9%)	≤ 2 years, 14 months, and 26 days

$$L_{void} = L^*(Void Volume). \tag{53}$$

By following Equation 54, L₂=24.625 mm is the effective length of UCFEC because 1.5% of the sample is the void volume. Using the interpolation between temperature variation 30°C and 60°C for da/dN, by applying the experimental data (Nakamura et al., 2007) mentioned previously, the da/dN= 1.133e-6 m/cycle for 50°C temperature variation between night and day on Mars is approximately obtained.

$$L_2 = L - L_{Void}, \tag{54}$$

$$\frac{da}{dN} N_f = 1, \tag{55}$$

By substituting the numerical values, L₂ = 24.625 mm and da/dN = 1.133e-6 m/cycle for ΔT = 50°C, in Equation 55, the fatigue life cycle numbers of UCFEC at 50°C temperature variation is approximated.

$$N_f = 21734 \text{ Cycles.}$$

21734 cycle numbers to fracture in UCFEC is the cycle numbers to fracture at zero inter laminar shear stress between carbon fiber and epoxy. Thus, due to the fact that except the 23°C temperature (crack free temperature), at other temperatures on Mars there is always inter laminar shear stress between carbon fiber and epoxy. Hence, at temperatures except 23°C, the fracture occurs in a condition that ILSS is equal to ILSS. It means that fracture occurs at numerical values less than N_f = 21734 cycles. As a result, based on this approach, the fatigue life of UCFEC on Mars can be approximated less than 21734 cycles.

RESULTS

The following results in Table 10 is obtained by the same analytical method earlier used in “Problem Formulation” to obtain the results and Equation 28 in vacuum thermal cycles fatigue in LEO simulation experiment; however, in this part of study, the steady-linear method to provide the Mars data is employed.

The following equation is derived by using the same method employed to derive Equation 28 in “Problem Formulation”. Equation 56 can be used to predict the thermal fatigue of UCFEC on Mars for 50°C temperature variation between night and day.

$$\frac{dD}{dN} = 2.397e-5 \Delta G^{5e-6}, \tag{56}$$

In Table 11, by using the Steady-linear method, the fatigue life of UCFEC in different seasons on Mars is approximated. Finally, the difference of cycle numbers to fracture between the steady-linear method and carbon fiber’s parallel crack propagation method is achieved.

DISCUSSION

In the present part of the research, the results obtained for crack density growth rate as a function of energy release rate, are compared with the results of a fatigue

Table 12. Comparison of crack density growth rate as a function of Energy Release Rate between [0₂/90₄]_s Fiberite 934/T300 composite and UCFEC in mechanical and LEO non-mechanical fatigue life experiment, respectively.

S/N	1	2	3	4	5	6	7
1	Crack density growth rate		1e-7	1e-6	1e-5	1e-4	1e-3
2	G_m , (J/m ²)	G_{m1} , [0 ₂ /90 ₄] _s 934/T300	285	421	610	930	1450
3		G_{m2} , Max, UCFEC	2.52	5.33	11.3	23.9	50.7
4	$\frac{G_{m1}}{G_{m2}}$		113	78.9	54	38.8	28.6
5	$\frac{G_{m1}}{G_{m2}} = \frac{\Delta\sigma_1 \cdot t_{934/T300's \text{ fibers}}}{\Delta\sigma_2 \cdot t_{UCFEC's \text{ fibers}}}$				53.8542		
6	Difference between experimental method data (row no. 4) and Equation (64) (%)		+110	+46.6	+0.23	-38.7	-88.4
7	Average difference between the experimental data and Equation (64) (%)				+5.987		

life experiment for [0₂/90₄]_s Fiberite 934/T300 composite under mechanical cyclic load $\Delta\sigma_1 = 188.4$ MPa. By using the data in Table 12, a relation for comparing the energy release rate between different fatigue life experiments is achieved. If the thickness of fibers in [0₂/90₄]_s Fiberite 934/T300 composite which has 6 fiber plies is considered 6 times of carbon fibers thickness in UCFEC which has 1 fiber ply; as a result, applying the following equations (by using Equations 57, 58, 60, and 62) (Maheswari and Prasad, 2013), to compare the energy release rate for different composites in fatigue life experiments under the different mechanical and non-mechanical cyclic loads, is proposed.

$$t_{934/T300's \text{ fibers}} = 6t_{UCFEC's \text{ fibers}} \quad (57)$$

For UCFEC exposed to thermal cyclic load, there are the following equations to understand the role of thermal stress and strain in the presented study.

$$\Delta l = l \cdot \Delta\alpha_l \cdot \Delta T, \quad (58)$$

$$\frac{\Delta l}{l} = \Delta\alpha_l \cdot \Delta T, \quad (59)$$

$$\frac{\Delta l}{l} = (\alpha_c - \alpha_l) \cdot (T_{\text{high}} - T_{\text{low}}), \quad (60)$$

$$\varepsilon = \Delta l / l, \quad (61)$$

$$\varepsilon = (\alpha_c - \alpha_l) \cdot (T_{\text{high}} - T_{\text{low}}), \quad (62)$$

$$\Delta\sigma_2 = \varepsilon \cdot G_c, \quad (63)$$

$$\Delta\sigma_2 = (\alpha_c - \alpha_l) \cdot (T_{\text{high}} - T_{\text{low}}) \cdot G_c, \quad (64)$$

Therefore, the following relation can be suggested to compare the energy release rate in different cyclic load conditions.

$$\frac{G_{m1}}{G_{m2}} = \frac{\Delta\sigma_1 \cdot t_{934/T300's \text{ fibers}}}{\Delta\sigma_2 \cdot t_{UCFEC's \text{ fibers}}}, \quad (65)$$

In the above Equations (57 to 64), α_c is epoxy coefficient of thermal expansion; α_l is carbon fiber axial coefficient of thermal expansion; G_c is epoxy shear modulus and ε is relative axial strain between epoxy and carbon fiber. In Figures, 18, 19, 20, 21, 22, and 23, crack density and crack density growth rate between [0₂/90₄]_s Fiberite 934/T300 and UCFEC due to fatigue, are compared. Furthermore, in Table 13 comparison of crack density growth rate as a function of energy release rate between [0₂/90₄]_s Fiberite 934/T300 composite and UCFEC in mechanical and non-mechanical fatigue life is indicated

Conclusion

In the presented research, by applying analytical methods and using experimental data, equations to predict the fatigue life of UCFEC in LEO and Mars environments are achieved. This material (UCFEC) is one of the materials that is applied in aerospace structures like space crafts and satellites. The fatigue life that is estimated by these approaches is due to non-mechanical fatigue which is thermal cycles. In a part of the study, convex curves method to predict the fatigue life in LEO simulation experiment is obtained. The results of convex curves method have indicated that the main reason for fracture of UCFEC in LEO environment is the degradation of inter laminar shear strength between the

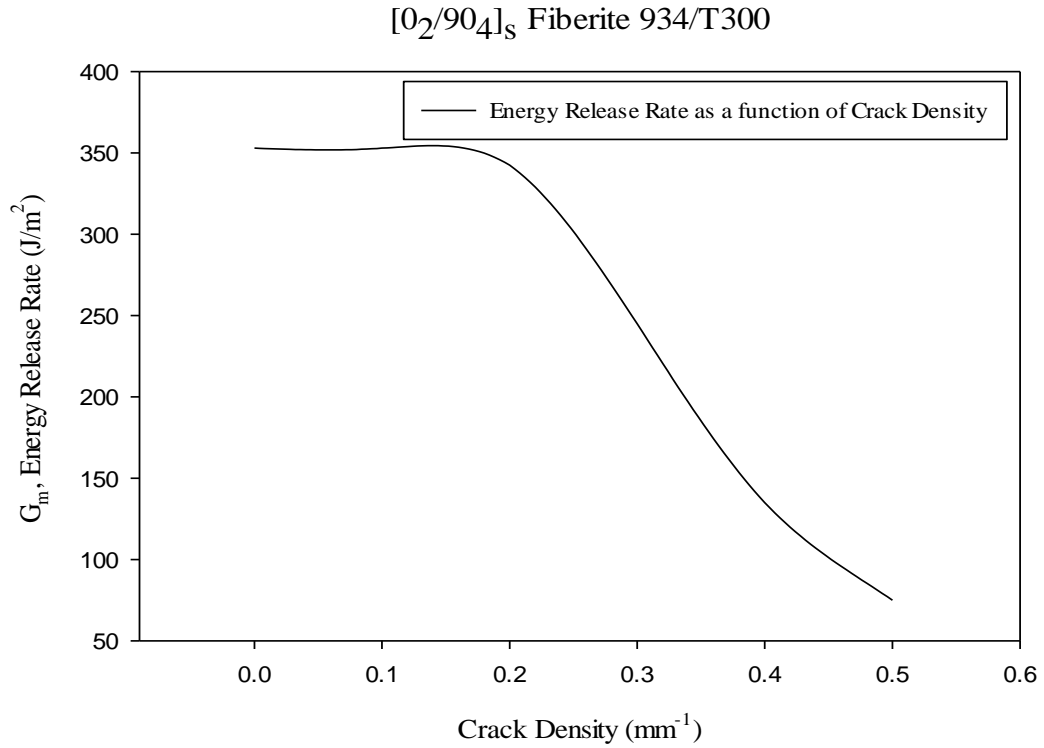


Figure 18. Energy release rate as a function of crack density for [0₂/90₄]_s Fiberite 934/T300 composite in fatigue life experiment under mechanical cyclic load $\Delta\sigma_1 = 188.4$ MPa.

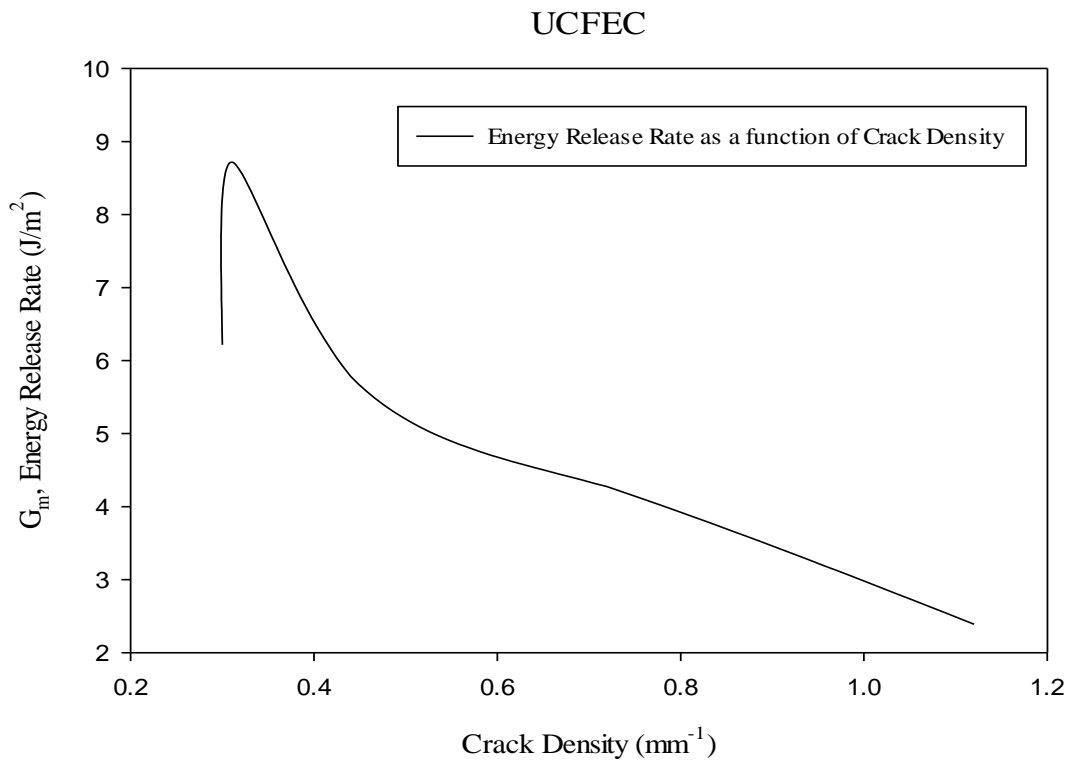


Figure 19. Energy release rate as a function of crack density for UCFEC in fatigue life experiment under non-mechanical cyclic load in LEO environment simulation experiment.

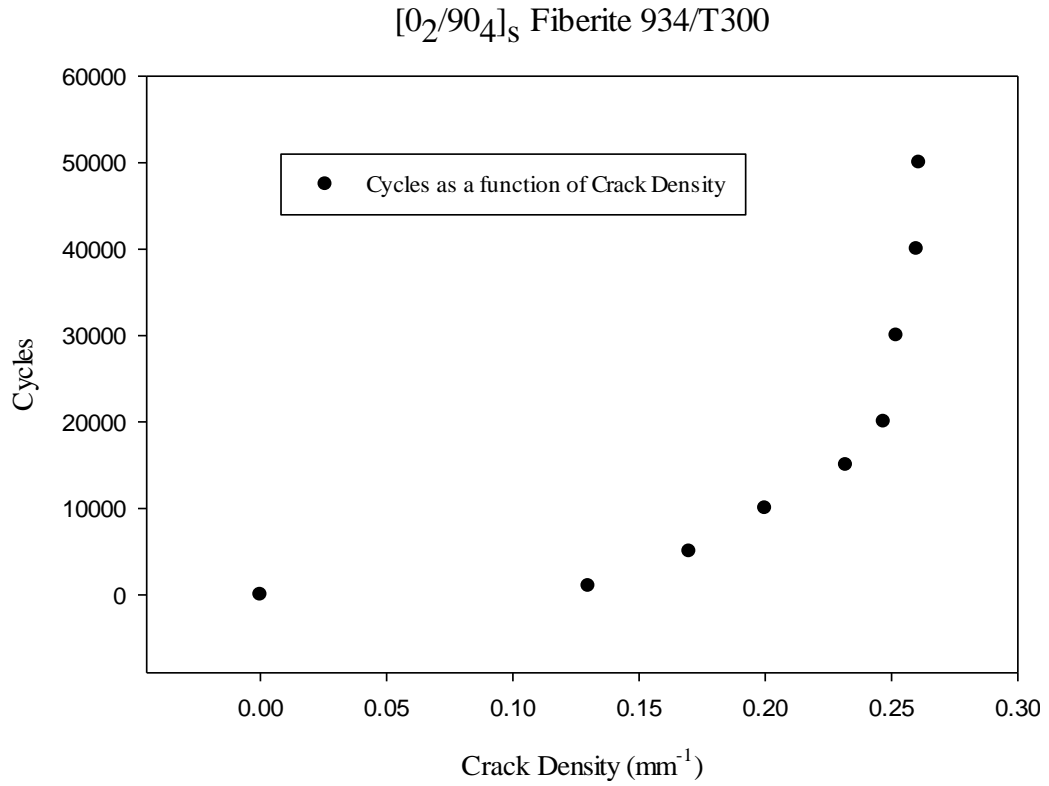


Figure 20. Cycle numbers as a function of crack density for $[0_2/90_4]_S$ Fiberite 934/T300 composite in fatigue life experiment under mechanical cyclic load $\Delta\sigma_1 = 188.4$ MPa.

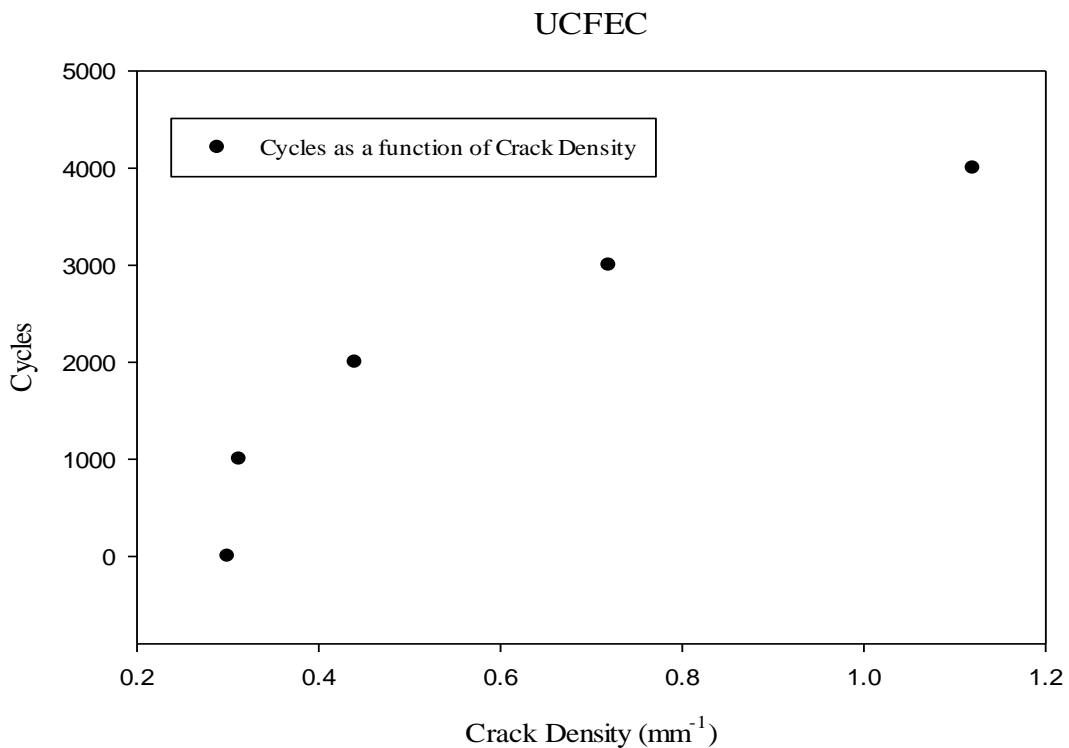


Figure 21. Cycle numbers as a function of crack density for UCFEC in fatigue life experiment under non-mechanical cyclic load in LEO environment simulation experiment.

[0₂/90₄]_s Fiberite 934/T300

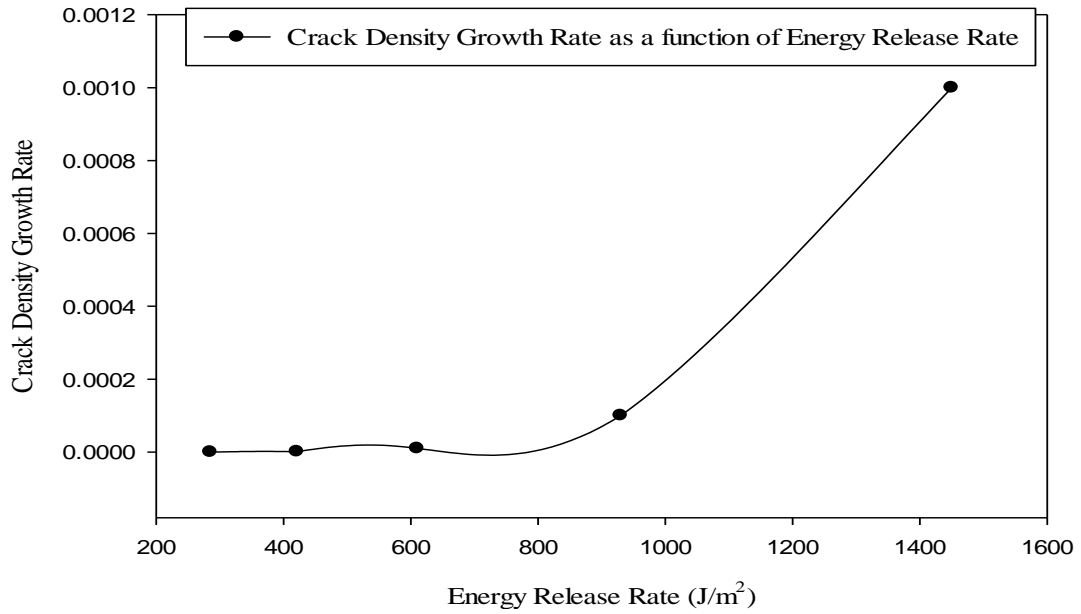


Figure 22. Crack density growth rate as a function of energy release rate for [0₂/90₄]_s Fiberite 934/T300 composite in fatigue life experiment under mechanical cyclic load $\Delta\sigma_1 = 188.4$ MPa.

UCFEC

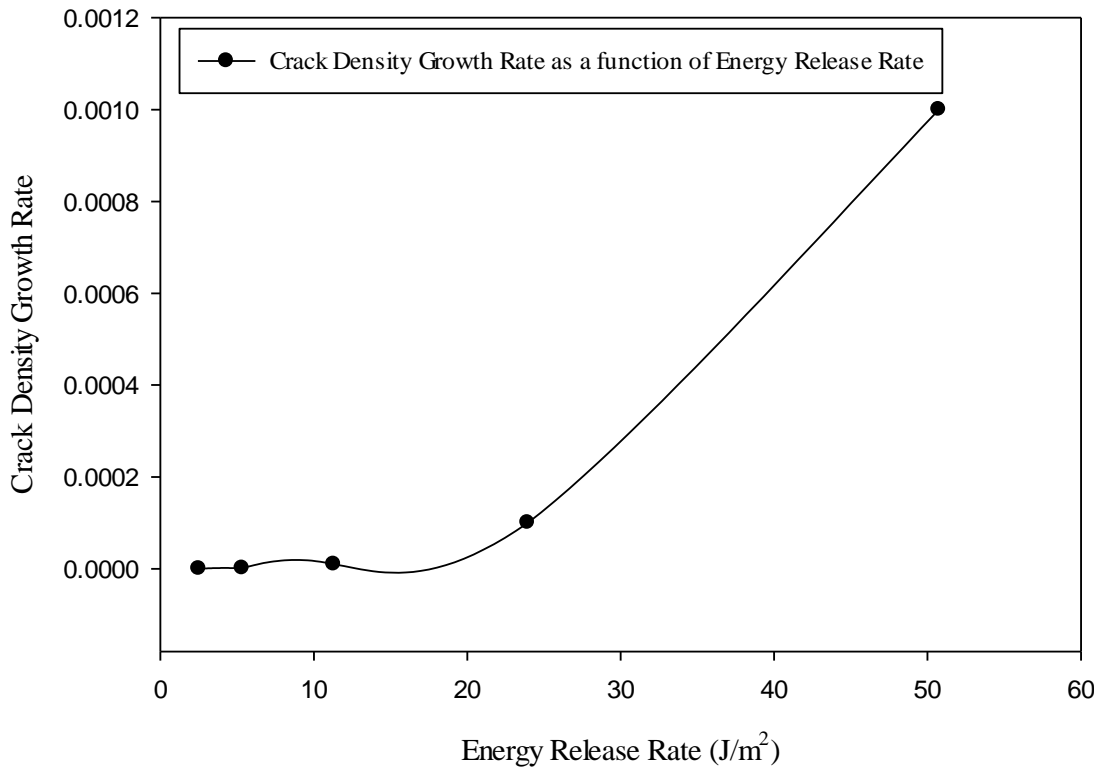


Figure 23. Crack density growth rate as a function of energy release rate for UCFEC in fatigue life experiment under non-mechanical cyclic load in LEO environment simulation experiment.

Table 13. Comparison of crack density growth rate as a function of energy release rate between [O₂/90₄]_s Fiberite 934/T300 composite and UCFEC in mechanical and non-mechanical fatigue life respectively.

Crack density growth rate	2.397e-5	1.976e-5
$G_{m1, \text{Fiberite, Experimental}} \cdot (\text{J/m}^2)$	660	650
$G_{m3, \text{Mars, } \Delta T = 50 \text{ }^\circ\text{C, Experimental}} \cdot (\text{J/m}^2)$	1	
$\frac{G_{m1, \text{Fiberite, Experimental}}}{G_{m3, \text{Mars, } \Delta T = 50 \text{ }^\circ\text{C, Experimental}}}$	660	
$\frac{G_{m1}}{G_{m3, \text{Mars, } \Delta T = 50 \text{ }^\circ\text{C}}} = \frac{\Delta \sigma_1 J_{934/T300's \text{ fibers}}}{\Delta \sigma_3 J_{\text{UCFEC's fibers}}}$	317.740	
Difference between experimental method data and Equation (64) between Fiberite composite and UCFEC on Mars at 50°C Temperature Variation (%)	+107.71	
Average difference between experimental method data and Equation (64) (%)	+75.458	

carbon fiber and epoxy. In addition, by inspiration of convex curves method, the steady-linear method to predict the fatigue life in Mars environment is achieved. The results of convex curves method, steady-linear method, and other fatigue experiments for composite materials are compared. The comparisons have shown that the fatigue life prediction results of UCFEC seem correct. The results that are achieved by steady-linear method have proved that the longest life of UCFEC on Mars occurs in Martian summer day environment, and shortest life occurs at Martian winter night.

For future work, the effect of Martian atmosphere on the fatigue life of UCFEC is highly recommended because in this research the vacuum condition is being considered. This is of high importance because the Mars atmosphere including gases, water vapor, and other factors, might have an increasing or decreasing effect on fatigue life of UCFEC in Mars environment. The presented study including the future work proposal can significantly play an important contributive role in the upcoming spacecraft's missions like the on-way human mission to Mars since predicting the thermal cyclic fatigue life is one of the most important issues that have to be considered for the space missions in order to achieve further space exploration.

CONFLICT OF INTERESTS

The author has not declared any conflict of interests.

ACKNOWLEDGEMENT

The author would like to appreciate the guidance of advisors. All the funding related to this study is provided by the presented author.

REFERENCES

- Anvari A (2014). Fatigue life prediction of unidirectional carbon fiber/epoxy composite in Earth orbit. *Int. J. Appl. Math. Mech.* 10(5):58-85.
- Anvari A (2016). Friction coefficient variation with sliding velocity in copper with copper contact. *Periodica Polytechnica, Mechanical Engineering.* 60(3):137.
- Anvari A (2017). Crack growth as a function of temperature variation in carbon fiber/epoxy. *J. Chem. Eng. Mater. Sci.* 8(3):17-30.
- Anvari A (2017). Effect of nano carbon percentage on properties of composite materials. *J. Chem. Eng. Mater. Sci.* 8(4):31-36.
- Anvari A (2017). Failure of Nickel-base super alloy (ME3) in aerospace gas turbine engines. *J. Chem. Eng. Mater. Sci.* 8(6):46-65.
- Adibnazari S, Anvari A (2017). Frictional effect on stress and displacement fields in contact region. *J. mech. eng. res.* 9(4):34-45.
- Biro T, Csizmadia J (2012). recent technique for thermal-fatigue simulation of heat-resistant steels. *periodica polytechnica, Mechanical Engineering.* 56(2):107-112.
- Diego A, Charles UR (2014). Symposium keynote: Enduring the isolation of interplanetary travel a personal account of the Mars500 mission. *Acta Astronautica.* 93:374-383.
- Des Marais DJ (2010). Exploring Mars for Evidence of Habitable Environments and Life. *Proceeding of the American philosophical society.* 154(4):402-422.
- Fujita K, Ozawa T, Okudaira K, Mikouchi T, Suzuki T, Takayanagi H, Tsuda Y, Ogawa, N, Tachibana S, Satoh T (2014). Conceptual study and key technology development for Mars Aeroflyby sample collection. *Acta Astronautica.* 93:84-93.
- Funk JG, Sykes GF (1989). The effects of simulated space environmental parameters on six commercially available composite materials. *NASA Technical Paper 2906.* Washington DC: National Aeronautics and Space Administration.
- Gao Y, He S, Yang D, Liu Y, Li Z (2005). Effect of vacuum thermo-cycling on physical properties of unidirectional M40J/AG-80 composites. *Compos. Part B: Eng.* 36:351-358.
- Giannadakis K, Varna J (2009). Effect of thermal aging and fatigue on failure resistance of aerospace composite materials. 5th International EEIGM/AMASE/FORGEMAT conference on Advanced Materials Research, IOP Conf. Series: Materials Science and Engineering 5, 012020:1-9. <http://dx.doi.org/10.1088/1757-899x/5/1/012020>.
- Guo W, Xue P, Yang J (2013). Nonlinear progressive damage model for composite laminates used for low-velocity impact. *Applied Mathematics and Mechanics (English Edition).* 34(9):1145-1154.
- Harris BED (2003). *Fatigue in Composites.* Woodhead Publishing Limited, Cambridge, UK.

- Hertzberg RW (1989). *Deformation and Fracture Mechanics of Engineering Materials*. Wiley. 467.
- Karadeniz ZH, Kumlutas D (2007). A numerical study on the thermal expansion coefficients of fiber reinforced composite materials. Master of science Thesis in mechanical engineering, Energy program, Dokuz Eylul University.
- Liu S, Nairn JA (1990). Fracture mechanics analysis of composite microcracking: Experimental results in fatigue. Proceeding of the 5th Technical Conference on Composite Materials, American Society of Composites, East Lansing, Michigan 6:287-295.
- Maheswari TS Uma, Prasad P Hari (2013). Reliability of Thermal strain and stresses in simple bars. *IOSR J. Math.* 5(2):05-09.
- Malekzadeh Fard K, Monfared MM, Norouzipour K (2013). Determination of stress intensity factor in half-plane containing several moving cracks. *Applied Mathematics and Mechanics (English Edition)*. 34(12):1535-1542.
- McEwen AS (2013). The surface of Mars changes all the time. Is flowing water one of the causes? *Scientific American*.
- Meszaros L, Turcsan T (2014). Development and mechanical properties of carbon fibre reinforced EP/VE hybrid composite systems. *periodica polytechnica, Mechanical Engineering*. 58(2):127-133.
- Mohlmann D, Thomsen K (2011). Properties of cryobrines on Mars. *Icarus*. 212:123-130.
- Nakamura T, Ramanujam N, Vaddadi P, Singh RP (2007). Interlaminar Fatigue Growth under Thermal Cycles in Composite Laminate. 16TH International Conference on Composite Materials, Kyoto, Japan.
- Pan SD, Zhou ZG, Wu LZ (2013). Basic solutions of multiple parallel symmetric mode-III cracks in functionally graded piezoelectric/piezomagnetic material plane. *Applied Mathematics and Mechanics (English Edition)*. 34(10):1201-1224.
- Park SY, Choi HS, Choi WJ, Kwon H (2012). Effect of vacuum thermal cyclic exposures on unidirectional carbon fiber/epoxy composites for low earth orbit space applications. *Composites: Part B*. 43:726-738.
- Pasachoff JM (1993). *From the Earth to the Universe. Part 2: The Solar System, 11 Mars*, Saunders College Publishing, Williamstown, Massachusetts, Fourth Edition, 190-203.
- Salotti JM (2011). Simplified scenario for manned Mars missions. *Acta Astronautica*. 69:266-279.
- Salotti JM (2012). Revised scenario for human missions to Mars. *Acta Astronautica*. 81(1):273-287.
- Suhir E (2012). Human-in-the-loop: likelihood of vehicular mission-success-and-safety. *J. Aircr.* 49(1):29-36.
- Salotti JM, Suhir E (2014). Manned missions to Mars: Minimizing risks of failure. *Acta Astronautica*. 93:148-161.
- Schulze-Makuch D, Davies P (2010). To Boldly Go: A One-Way Human Mission to Mars. *J. Cosmology*. 12:3619-3626.
- Shin KB, Kim CG, Hong CS, Lee HH (2000). Prediction of failure thermal cycles in graphite/epoxy composite materials under simulated low earth orbit environments. *Compos Part B: Eng.* 31:223-235.
- Song K, Zhang Y, Meng J, Green EC, Tajaddod N, Li H, Minus ML (2013). Structural Polymer-Based Carbon Nanotube Composite Fibers: Understanding the Processing Structure-Performance Relationship. *Materials*. 6:2543-2577.
- Sendeckyj GP (1990). Life prediction for resin-matrix composite materials, (Reifsnider, K.L., editor). *Fatigue of Composite Materials*. Elsevier Science Publishers, 431-483.
- Uleck KR (2006). A Hybrid Model for Fatigue Life Estimation of Polymer Matrix Composites. Ph.D. thesis, University of Maryland: 108.
- Voicu R (2012). Structural Characterization and Mechanical Behaviour of Carbon Fiber/epoxy Composite for Aeronautical Field. *Materiale Plastice*. 49(1):34-40.

Full Length Research Paper

Thermal fatigue life of carbon nanotube wire and unidirectional carbon fiber/epoxy composite (UCFEC) in earth orbit

A. Anvari

Department of Mechanical and Aerospace Engineering, University of Missouri-Columbia, Columbia, Missouri, U.S.A.

Received 6 September, 2017; Accepted 20 October, 2017

The most important target of this study is to develop a method to compare the materials' degradation due to thermal fatigue and temperature variation between the carbon nanotube wire and unidirectional carbon fiber/epoxy composite (UCFEC). In the presented study, by using experimental results data, thermal fatigue life of carbon nanotube wire and unidirectional carbon fiber/epoxy was compared after being exposed to temperature variation in space. This process was done by using a new analytical method that models the material strength deterioration as a function of temperature variation in low Earth orbit thermal cycles. Based on the relations that were obtained by using recommended analytical method, the carbon nanotube wire offered less thermal fatigue strength degradation equal to 6.608% after being subjected to 1,200,000°C temperature variation in comparison with unidirectional carbon fiber/epoxy composite thermal fatigue strength degradation. Therefore, it seems that carbon nanotube wire shows better thermal fatigue resistance. The results of this comparison may be used to determine the suitable carbon material for space missions based on thermal fatigue life.

Key words: Carbon nanotube, low earth orbit, thermal cycles, temperature variation, material degradation.

INTRODUCTION

Polymer materials can be used in many applications such as films, fibers, sheets, and coatings (Song et al., 2013). These forms may be applied to produce clothing, carpets, ropes, and reinforcements (Song et al., 2013). In application of carbon and nanomaterial, a few works are submitted by Saleh (2016, 2017, 2018), Saleh et al. (2017), and Gaddafi and Saleh (2017). Among the characteristics of carbon fibers, low densities, high thermal and chemical stabilities can be mentioned (Huang, 2009). This material can be applied in many industries such as aerospace, turbine blades, etc. Other characteristics of these materials are high strength and

lightweight (Wilkerson et al., 2007). Furthermore, carbon fibers may be applied in composites to manufacture the flaps, aileron, and landing gear doors (Voicu, 2012). Further investigation on composite materials properties are also performed by Chow et al. (2016), Meszaros and Turcsan (2014), and Jo and Lee (2014).

Recently, unidirectional carbon fiber/epoxy composite (UCFEC) and carbon nanotube (CNT) wire have been applied in many industries like aerospace. To make sure that the aerospace structure is safe and reliable, fatigue life of UCFEC and CNT wire in space needs to be estimated because thermal fatigue in space is one of the

E-mail: aabm9@mail.missouri.edu.

Author(s) agree that this article remain permanently open access under the terms of the [Creative Commons Attribution License 4.0 International License](https://creativecommons.org/licenses/by/4.0/)

important issues that affects space structures.

Thermal fatigue occurs while thermal cycles exist. A great example for thermal fatigue in space is satellite that rotates around the planets. These satellites while rotating around the planets pass through the planets' shadows which may be extremely cold, and sun illumination which is extremely hot. As a result of the full rotation around the planet, a thermal cycle appears to affect the structure. These thermal cycles may cause crack initiation and propagation in aerospace structures. Thus, thermal fatigue analysis of space structures is really important to prevent crack initiation, propagation, and fracture in space environment. In order to predict the long-term durability, recently, "crack closure detection using photometrical analysis is submitted by Savkin et al. (2015) and "durability and integrity studies of environmentally conditioned interfaces in fibrous polymeric composite: critical concepts and comments" is provided by Ray and Rathore (2014).

In assessment of the damage in different materials, "canary approach for monitoring BGA interconnect reliability under temperature cycling" is presented by Chauhan et al. (2012), "thermal fatigue and hypothermal atomic oxygen exposure behavior of carbon nanotube wire" is provided by Misak et al. (2013), and "determination of material parameters for discrete damage mechanics analysis of carbon-epoxy laminates" is developed by Barbero and Cosso (2014). Furthermore, in the area of obtaining analytical evaluation methods for determining mechanical properties of different materials, a few works are submitted by Anvari (2014, 2016a, b, 2017a, b, c) and Adibnazari and Anvari (2017).

Some of the cited studies have investigated the fatigue life of composite laminates. Nevertheless, it appears that there are a few works in this area that can clearly illustrate the thermal deterioration in CNT wire and UCFEC. In addition, it seems that there is no work to compare the thermal fatigue life of these two materials in space.

In the presented research, by applying two experimental procedures and using a new analytical method, relations to predict the strength degradation of UCFEC in various temperature variations are achieved. By using these relations, material strength degradation between CNT wire and UCFEC is compared. The results of this contribution can also be applied for estimation of strength of UCFEC in different temperature variations. Therefore, this analytical method might be helpful to predict the thermal life of UCFEC in space environment, especially in low earth orbit environment. In this study, the thermal resistance of UCFEC and CNT wire in low earth orbit is measured and compared with each other. It seems that this method is a novel approach of comparison since it has not been used in any other works. According to this approach, material degradation is measured based on temperature variation which is applied to estimate the thermal fatigue life.

EXPERIMENTAL PROCEDURES

The experimental procedure (Park et al., 2012) that is mentioned in this study simulates the Low Earth Orbit (LEO) environment as satellite rotates around the earth as is illustrated in Figure 1. In this experiment, polyacrylonitrile (PAN)-based unidirectional Torayca carbon fibers in the form of prepeg tape is used (Park et al., 2012). The laminated composite panels were fabricated by stacking multiple layers of unidirectional prepregs. All prepregs had zero degree orientation at normal thicknesses of 1.0, 1.5 and 3.0 mm. Cure temperature and cycle times were 176.7°C for 180 min. A consolidation pressure was employed throughout the cure cycles with a full vacuum of 1 bar (107.9 kPa) (Park et al., 2012). The experiment was performed in an environmental chamber with a proportional integral derivative (PID) programmable temperature controller. Test temperature range should be as large as possible to meet environmental stress screening (ESS) purposes based on the guideline in MIL-STD-810F (Park et al., 2012). This environment consists of vacuum thermal cycles of 120°C to -175°C and back to 120°C (Park et al., 2012). 120°C is related to sun illumination and -175°C is related to solar eclipse (Park et al., 2012). For investigation of UCFEC mechanical properties deterioration due to low earth environment condition, 2000 thermal cycles have been performed in laboratory (Park et al., 2012). After this experiment, samples were cut and then dried in a vacuum oven at 60°C for 24 h to remove moisture (Park et al., 2012). The standard temperature and relative humidity used in this laboratory are $23 \pm 2^\circ\text{C}$ and $50 \pm 5\%$, respectively (Park et al., 2012). The sample dimensions for static mechanical tests are shown in Figure 3.

In UCFEC sample, all the carbon fibers are parallel imbedded in epoxy. The UCFEC sample is illustrated in Figure 2 (Park et al., 2012). In the following sections, the analytical method used to estimate the crack propagation of UCFEC in LEO environment is discussed.

Void volume in UCFEC after being exposed to 0, 500, 1000, 1500, and 2000 thermal cycles is indicated in Table 2. With the application of data in Table 2, equation to estimate the void volume in UCFEC after being exposed to thermal cycles in LEO can be obtained. Furthermore, by application of derivative on void volume with respect to cycle numbers, void volume growth rate may be obtained. Due to this fact that in this experiment void volume growth occurs as a result of crack growth, this derivative may be able to predict crack growth rate in UCFEC sample in LEO environment.

$$V_{\text{void}} = aN^2 + bN + c \quad (1)$$

At the beginning of the simulation experiment (0 cycles), the void volume percent is equal to 0.015, therefore

$$0.015 = a(0)^2 + b(0) + c \quad (2)$$

and at 1000 cycle, void volume percent is equal to 0.0166, thus

$$0.01798 = a(1000)^2 + b(1000) + c \quad (3)$$

Furthermore, at 2000 cycles, the void volume percent in sample is, 0.0228. As a result

$$0.02352 = a(2000)^2 + b(2000) + c \quad (4)$$

Thus, by solving the three equations ((2), (3), and (4)), three unknown quantities (a , b , and c), equation (5) is obtained that indicates the void volume percent in sample as a function of the

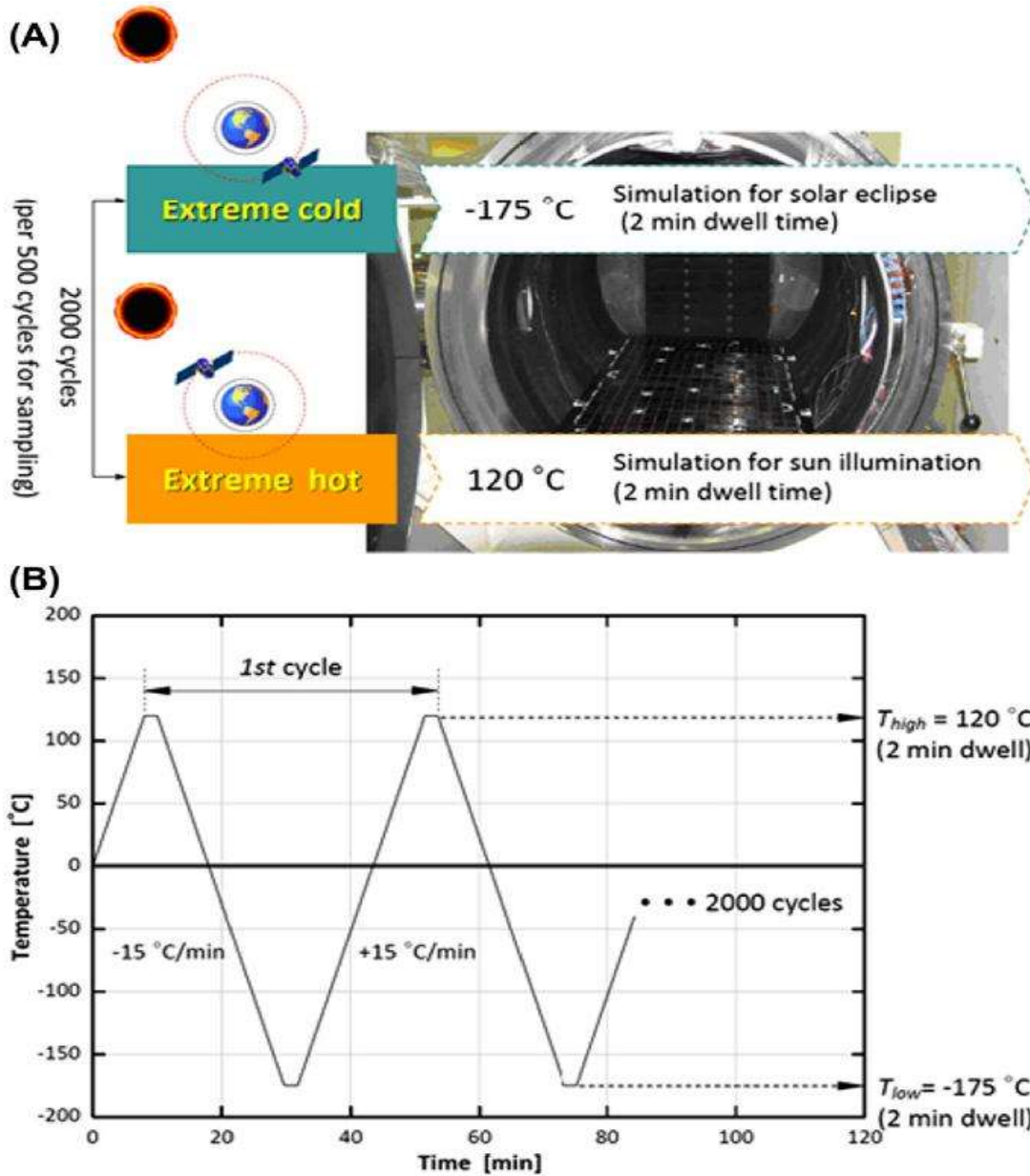


Figure 1. Vacuum thermal cycling test for the LEO space environment simulation: (A) thermal vacuum chamber; and (B) thermal cycling temperature profiles. Source: Park et al. (2012).

cycle numbers. In Figure 4, void volume to total volume ratio in sample as a function of Cycle numbers in LEO simulation experiment is illustrated:

$$V_{\text{void}} = (1.28e - 9)N^2 + (1.7e - 6)N + 0.015 \quad (5)$$

With the application of equation (5), obtaining void volume in any cycle number is possible. As an instance, in 3,000 and 4,000 thermal cycles, the void volume is equal to 0.03162 and 0.04228, respectively. By using partial derivative on equation (5), crack density growth rate estimation equation is obtained. The results of this derivative are indicated in equations (6) and (7).

$$\frac{dV_{\text{void}}}{dN} = (2.56e - 9)N + 1.7e - 6 \quad (6)$$

$$\frac{dV_{\text{void}}}{dN} = \frac{dD}{dN} = (2.56e - 9)N + 1.7e - 6. \quad (7)$$

Continuing this approach and using the data in Table 2, a, which is the crack length equation as a function of thermal cycles is obtained. In this study, void volume percent is equal to crack length percent because the voids are induced due to the crack growth.

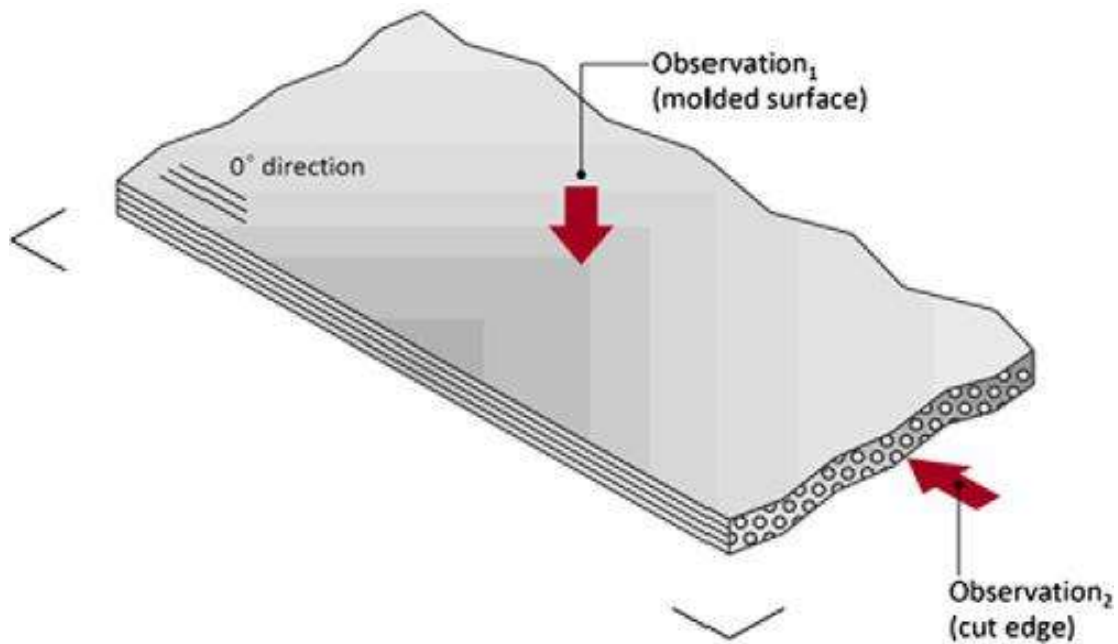


Figure 2. Microscopic observation of unidirectional carbon fiber/epoxy laminates exposed to vacuum thermal cycling.
Source: Park et al. (2012).

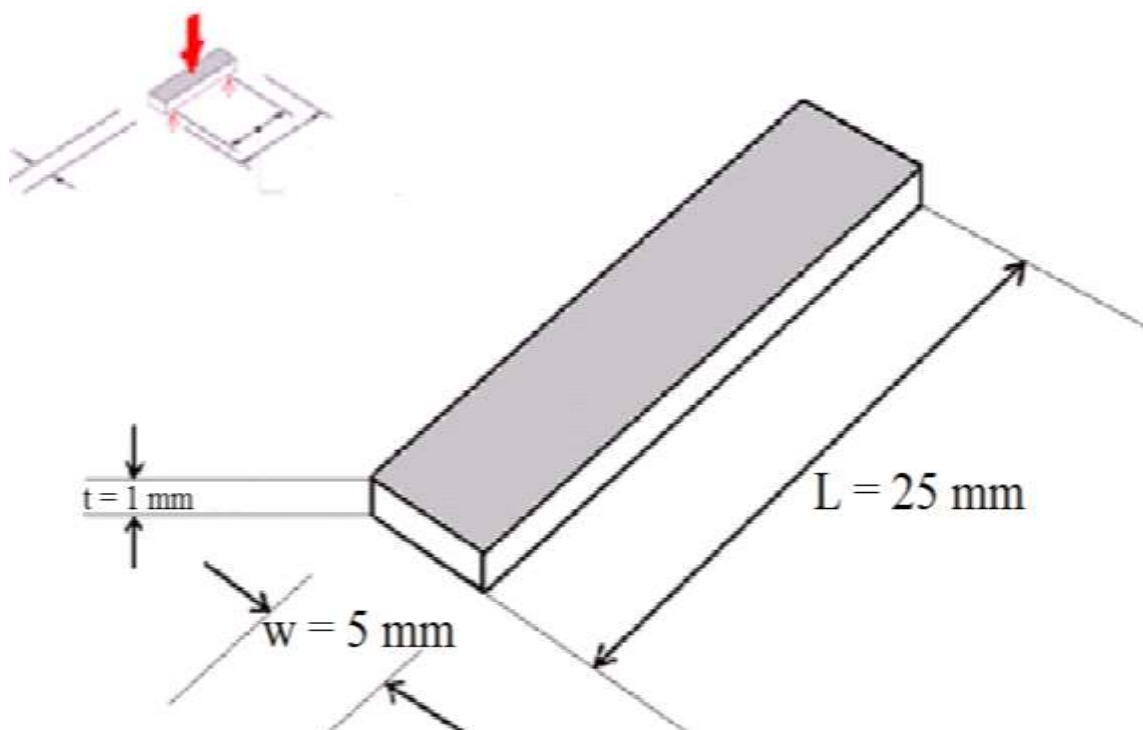


Figure 3. Sample dimensions (units: mm) for static mechanical tests: (A) ILSS, ASTM D 2344.
Source: Park et al. (2012).

$$a = (3.1966e-8)N^2 + (4.2534e-5)N + 0.375,$$

(8) Thus, the crack growth rate relation can be defined as:

UCFEC

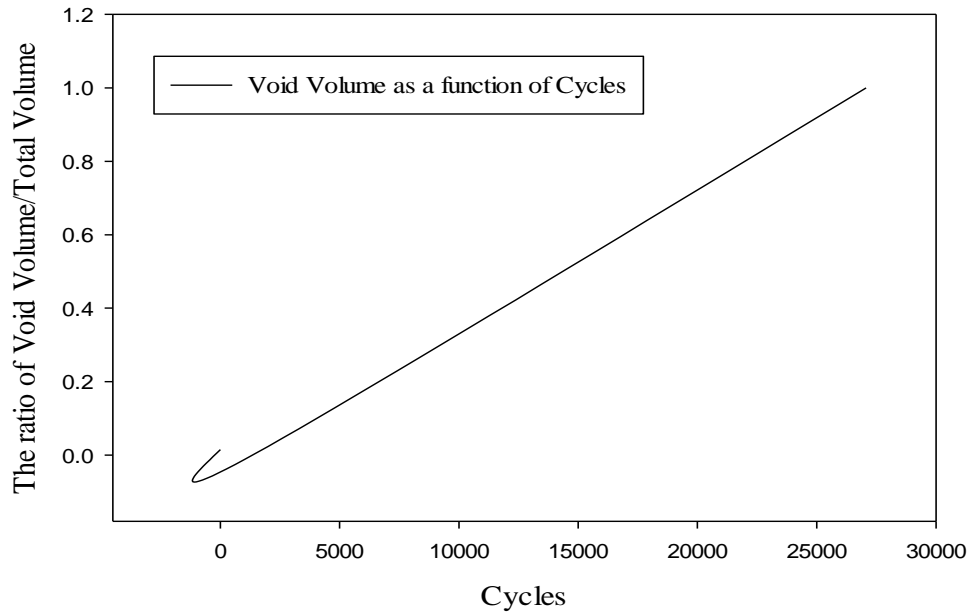


Figure 4. Void volume to total volume ratio in sample as a function of cycle numbers in LEO simulation experiment.

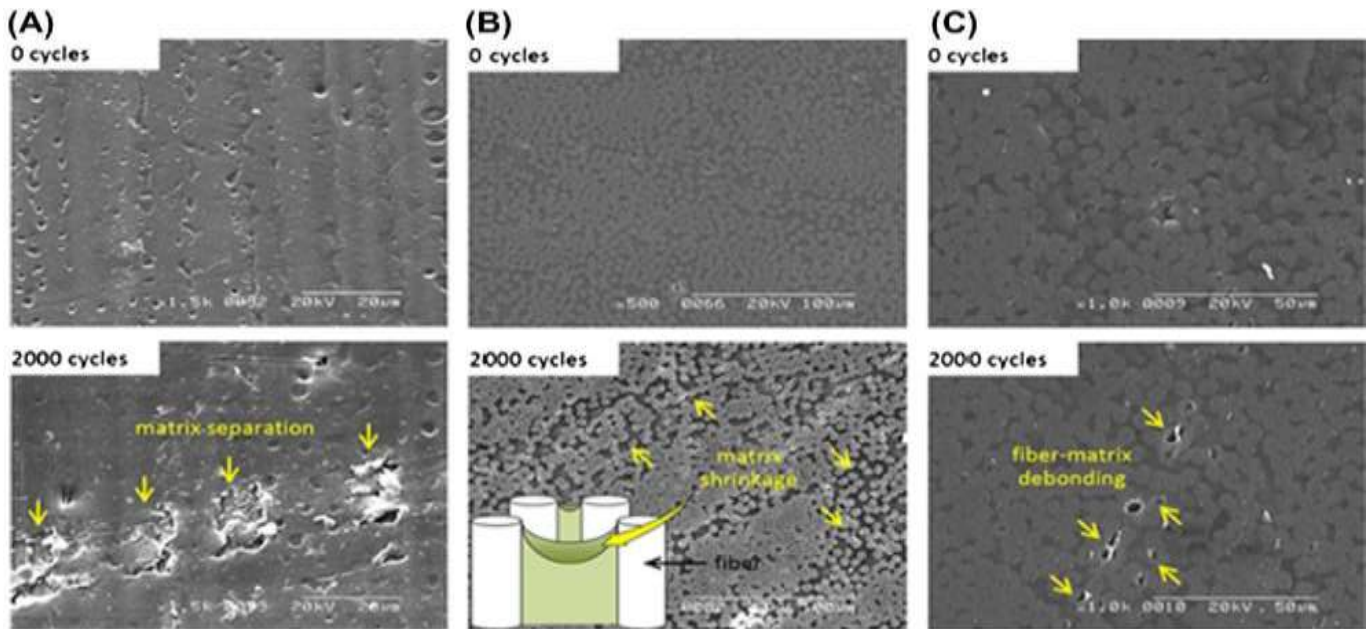


Figure 5. Electron micrographs showing different types of damage before and after vacuum thermal cycling: (A) laminate surface at 1500 × magnification showing matrix separation; (B) cross-sectional view at 500 × magnification showing matrix shrinkage; and (C) cross-sectional view at 1000 × magnification showing fiber-epoxy matrix debonding. Source: Park et al. (2012).

$$\frac{da}{dN} = (6.3932e-8)N + (4.2534e-5)$$

(9)

Because each cycle is temperature variation from 120 to -175°C and back to 120°C (Karadeniz, 2005), as a result, each cycle is equal to 590°C temperature variation. Thus, 1°C temperature

Table 1. Material properties of UCFEC.

Materials	Epoxy	Carbon fiber
Axial coefficient of thermal expansion (CTE), ($1/^{\circ}\text{C}$)	43.92e-6	-0.83e-6
Transverse coefficient of thermal expansion (CTE), ($1/^{\circ}\text{C}$)	43.92e-6	6.84e-6
Axial Poisson's ratio	0.37	0.20
Transverse Poisson's ratio	0.37	0.40
Axial elastic modulus, (GPa)	4.35	377
Transverse elastic modulus, (GPa)	4.35	6.21
Axial shear modulus, (GPa)	1.59	7.59
Transverse shear modulus (GPa)	1.59	2.21
Thickness, (mm)	0.50	0.50

Source: Park et al. (2012) and Karadeniz (2005).

Table 2. Void volume property and crack length results of UCFEC (M40J) as a function of vacuum thermal cycling: $E(x) \pm V(x)$.

a (Crack Length) (mm)	0.3750	0.4075	0.4150	0.4800	0.5700
V_{void} , (%)	1.50 ± 0.25	1.63 ± 0.31	1.66 ± 0.42	1.92 ± 0.51	2.28 ± 0.84
Cycles	0	500	1000	1500	2000

Source: Park et al. (2012).

variation is 1/590 of each cycle. In addition, Δt Celsius temperature variation may be determined as $\Delta t/590$.

By imposing this result into equation (8), equation (10) can be achieved. Equation (10) indicates the crack length as a function of temperature variation.

$$a = (3.1966e - 8) \left(\frac{\Delta t_{\text{total}}}{590} \right)^2 + (4.2534e - 5) \left(\frac{\Delta t_{\text{total}}}{590} \right) + 0.375 \quad (10)$$

Moreover, because 590 is the temperature variation at Earth Orbit Cycle (EOC), therefore, it can be named as Δt_{EOC} . By substituting Δt_{EOC} into equation (10), the following equation (11) is obtained.

$$a = (3.1966e - 8) \left(\frac{\Delta t_{\text{total}}}{\Delta t_{\text{EOC}}} \right)^2 + (4.2534e - 5) \left(\frac{\Delta t_{\text{total}}}{\Delta t_{\text{EOC}}} \right) + 0.375. \quad (11)$$

In Figure 5, UCFEC before and after being exposed to 2000 thermal cycles in earth orbit is illustrated. In sections A, B, and C of Figure 5, matrix separation, matrix shrinkage, and matrix de-bonding are shown, respectively. Matrix separation and fiber-matrix de-bonding can induce deterioration in UCFEC that may cause crack initiation, propagation and fracture due to thermal fatigue.

Convex curves method with application of least square approach

In this section, a method is introduced to estimate the thermal fatigue life of UCFEC in LEO environment condition. The data used

to develop the equations representing convex curves (Anvari, 2014) with applying least square method, are exploited from an experimental procedure (Park et al., 2012). As it can be observed in Table 1, the amount of CTE values in carbon fiber is different from epoxy. This difference of CTEs between these two materials may cause different values of strain once the UCFEC is being heated or cooled. This difference of strains may cause interface stress between carbon fiber and epoxy. This process can lead to matrix separation or fiber-matrix de-bonding that cause deterioration in UCFEC due to thermal fatigue. In Table 3, functions that are obtained to determine the fatigue life cycles of UCFEC in LEO environment simulation experiment are indicated.

RESULTS AND DISCUSSION

In the presented part of this study, the results of this research are compared with the results of another experiment (Misak et al., 2013). In the comparison of these two results, material strength as a function of temperature variation has been investigated. Both experiments are thermal fatigue experiments on UCFEC and CNT wire materials, respectively.

For the first experiment (Park et al., 2012), a procedure to achieve the material strength as a function of temperature variation is introduced in this section and for the second experiment (Misak et al., 2013), data for CNT wire strength in two states of as-received and after being exposed to 1,200,000 temperature variation (5000 thermal cycles in low Earth orbit) are available from the

Table 3. Functions that are obtained to determine the fatigue life cycles in LEO environment simulation experiment.

Equation name and number	Functions	Critical functions	Cycle No. to failure (N_f)
V_{void} (5)	$V_{void} = (1.28e - 9)N^2 + (1.7e - 6)N + 0.015$	$1 = (1.28e - 9)N^2 + (1.7e - 6)N + 0.015$	27070
FM, (MPa) (12)	$FM = (-5.35e - 6)N^2 - (0.01491)N + 199.8$	$0 = (-5.35e - 6)N^2 - (0.01491)N + 199.8$	4874
ILSS, (MPa) (13)	$ILSS = (-1.05e - 6)N^2 - (4.41e - 3)N + 80.9$	$0 = (-1.05e - 6)N^2 - (4.41e - 3)N + 80.9$	6925
FS, (MPa) (14)	$FS = (-9.55e - 6)N^2 - (0.07825)N + 1368.6$	$0 = (-9.55e - 6)N^2 - (0.07825)N + 1368.6$	8555

Source: Anvari (2014).

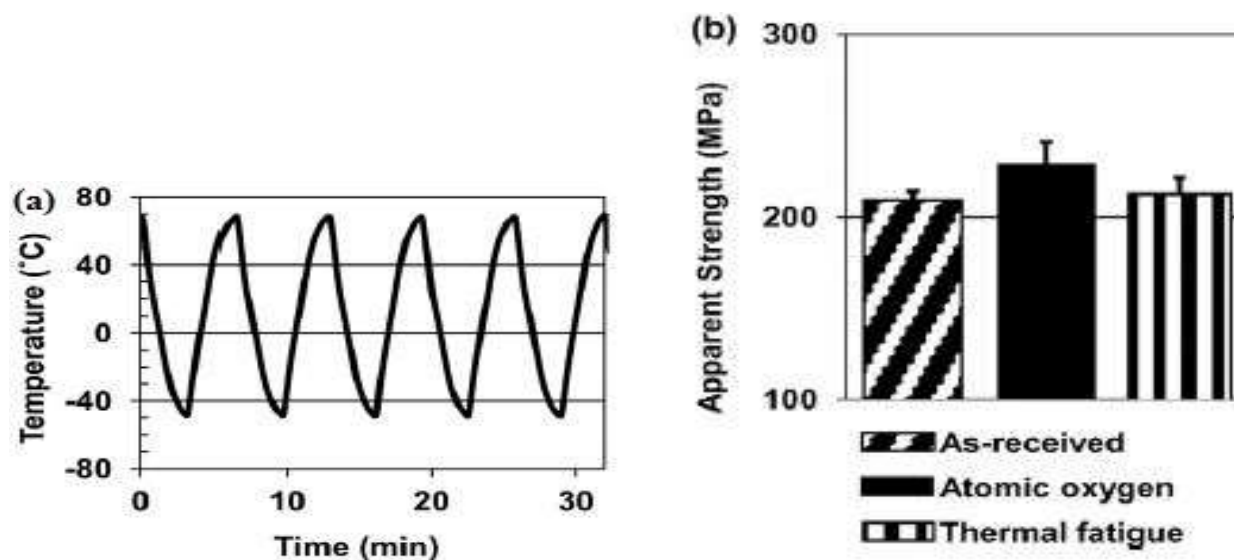


Figure 6. Temperature variation in low Earth orbit thermal cycles simulation experiment on CNT wire (a) and apparent strength of CNT wire before and after this experiment. Source: Misak et al. (2013).

experiment data (Misak et al., 2013). In Figure 6(b) (Misak et al., 2013), the remaining apparent strength for CNT wire after 5,000 thermal cycles

with 240°C temperature variation at each of cycles is illustrated. It seems that after these cycles, apparent strength of CNT wire is decreased from

about 227 to 212 Mpa. That is 6.608% decrease in apparent strength.

In order to convert these cycles to temperature

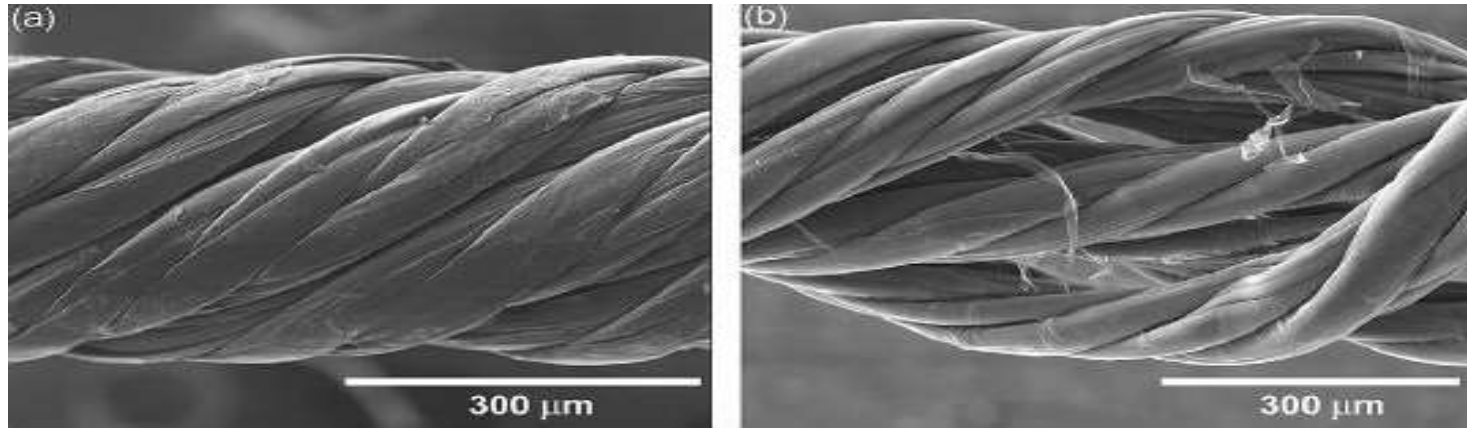


Figure 7. CNT wire used in low earth orbit environmental condition (a) As-received CNT wire and (b) after fracture. Source: Misak et al. (2013).

variation, the following relation can be used: $\Delta t_{total} = \Delta t \cdot N$, where Δt_{total} is the total temperature variations after the experiment, Δt is the temperature variation at each cycle (240°C temperature variation for the CNT wire experiment (Misak et al., 2013)) and N is the number of cycles for the experiment (5,000 cycles for the CNT wire experiment (Misak et al., 2013)). By using these assumptions and based on the mentioned relation, the total temperature variations after the thermal fatigue experiment becomes: $240 \cdot 5000$, that is equal to 1,200,000 temperature variations. In Figure 7, CNT wire used in low earth orbit environmental condition is shown.

The numerical quantity of Δt_{total} that is obtained from the mentioned relation can be substituted into the following equations to predict the strength of UCFEC in first thermal fatigue experiment (Park et al., 2012). The amounts that are obtained from these relations can be applied to compare the results between the two thermal fatigue experiments. As it is obvious, this relation can contribute to compare the strength of CNT wire

and UCFEC after being subjected to 1,200,000 temperature variations in low Earth orbit environment condition. Because each Earth orbit cycle is 590°C temperature variation in UCFEC experiment (Park et al., 2012), therefore, $N = \Delta t_{total} / 590$. By substituting this relation into equations (12), (13), and (14), equations (15), (16), and (17) are achieved and can be used to compare the strength between the CNT wire and UCFEC after being exposed to 1,200,000 total temperature variations. The comparison results are indicated in Table 4. Moreover, as-received and thermal fatigued CNT wire are illustrated in Figures 8 and 9 (Misak et al., 2013).

$$FM = (-5.35e-6)\left(\frac{\Delta t_{total}}{590}\right)^2 - (0.01491)\left(\frac{\Delta t_{total}}{590}\right) + 199.8 \quad (15)$$

$$ILSS = (-1.05e-6)\left(\frac{\Delta t_{total}}{590}\right)^2 - (4.41e-3)\left(\frac{\Delta t_{total}}{590}\right) + 80.9 \quad (16)$$

$$FS = (-9.55e-6)\left(\frac{\Delta t_{total}}{590}\right)^2 - (0.07825)\left(\frac{\Delta t_{total}}{590}\right) + 1368.6 \quad (17)$$

Conclusion

In the presented research, by using two experimental procedures data that have been performed on UCFEC and CNT wire, and a new analytical method with the application of least square approach, equations are obtained to compare the material strength between the CNT wire and UCFEC after being subjected to vacuum thermal cycles in low Earth orbit environment simulation condition. The results of this study have indicated that after 1,200,000°C temperature variation in this condition, UCFEC has shown the average 9.568% more material strength degradation in comparison with CNT wire. Based on this process, it appears that CNT wire is a more durable material in vacuum thermal cycle's conditions and UCFEC exhibits less strength stability in this environment condition. Therefore, it seems that CNT wire can represent a more life in low Earth orbit environment condition. Nevertheless, more analysis may be required to compare that which one of these materials are more cost-effective in

Table 4. Comparison of material strength degradation between UCFEC and CNT wire as a result of temperature variations from two thermal fatigue experiments of low Earth orbit simulation environment.

Material condition	Material strength (Mpa)	Decrease percent in material strength after being subjected to temperature variation
UCFEC at zero temperature variation	ILSS = 80.900 [25]	0
	FS = 1368.600 [25]	0
	FM = 199.800 [25]	0
CNT wire at zero temperature variation	227 [27]	0
UCFEC after being exposed to 1,200,000°C temperature variation	ILSS = 68.564	15.248%
	FS = 1224.187	10.552%
	FM = 154.391	22.787%
	Average of ILSS, FS, and FM reduction percent = 16.176%	
CNT wire after being exposed to 1,200,000°C temperature variation	212 [27]	6.608%
Difference between materials strength of CNT wire and UCFEC after being subjected to 1,200,000 temperature variation	9.568%	

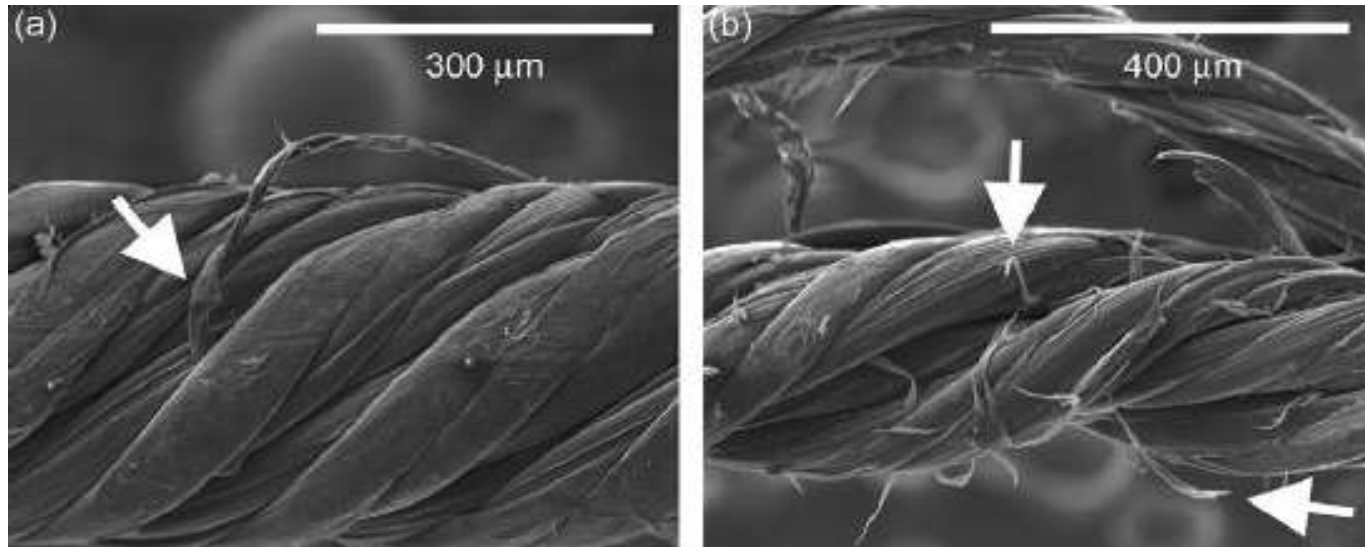


Figure 8. CNT wire (a) after thermal fatigue used in low earth orbit environmental condition with fractured CNT bundles (white arrow) and (b) after thermal fatigue and tensile test having fraying appearance (white arrow). Source: Misak et al. (2013).

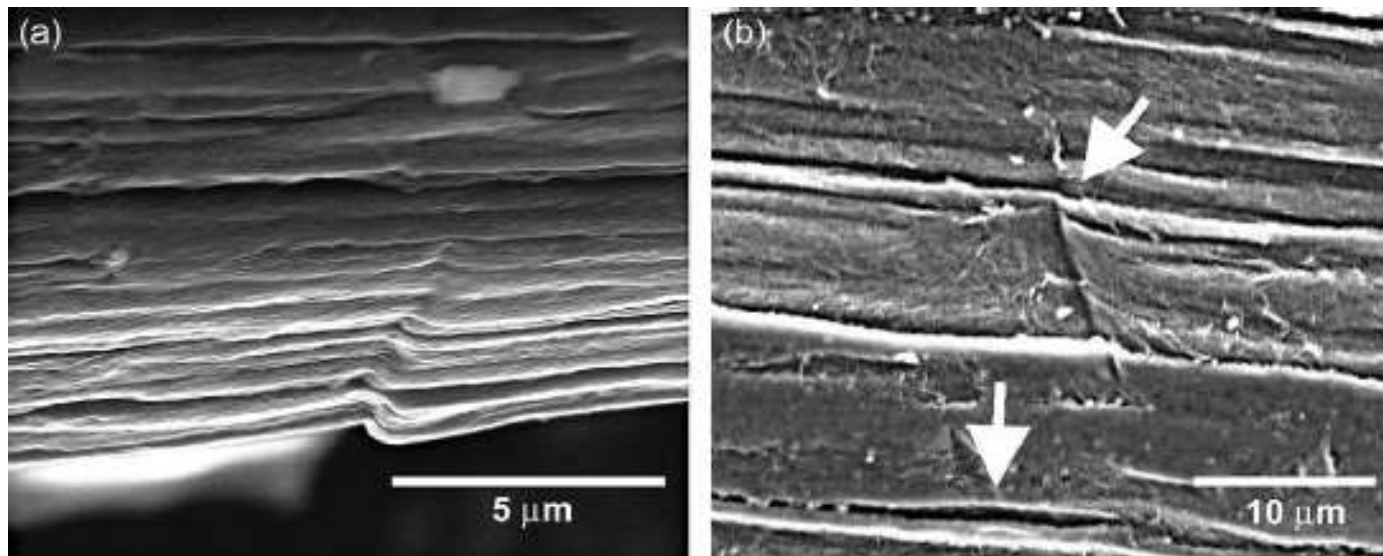


Figure 9. Thermal fatigued CNT wire used in low earth orbit environmental condition (a) kink band formation and (b) delamination (lower arrow) and crack formation (upper arrow).
Source: Misak et al. (2013).

different aerospace missions that they encounter to temperature variation cycles.

CONFLICT OF INTERESTS

The author has not declared any conflict of interests.

ACKNOWLEDGEMENT

The author would like to appreciate the guidance of advisors. All the funding related to this research is provided by the presented author.

REFERENCES

- Aadibnazari S, Anvari A (2017). Frictional effect on stress and displacement fields in contact region. *J. Mech. Eng. Res.* 9(4):34-45.
- Anvari A (2014). Fatigue life prediction of unidirectional carbon fiber/epoxy composite in Earth orbit. *Int. J. Appl. Math. Mech.* 10(5):58-85.
- Anvari A (2016). Fatigue life of unidirectional carbon fiber/epoxy in Earth orbit and Mars. 33rd annual RCAF conference, University of Missouri-Columbia, U.S.A.
- Anvari A (2016). Friction coefficient variation with sliding velocity in copper with copper contact. *Periodica Polytechnica, Mech. Eng.* 60(3):137.
- Anvari A (2017). Crack growth as a function of temperature variation in carbon fiber/epoxy. *J. Chem. Eng. Mater. Sci.* 8(3):17-30.
- Anvari A (2017). Effect of nano carbon percentage on properties of composite materials. *J. Chem. Eng. Mater. Sci.* 8(4):31-36.
- Anvari A (2017). Failure of Nickel-base super alloy (ME3) in aerospace gas turbine engines. *J. Chem. Eng. Mater. Sci.* 8(6):46-65.
- Barbero EJ, Cosso FA (2014). Determination of Material Parameters for Discrete Damage Mechanics Analysis of Carbon-Epoxy Laminates. *Composites: Part B* 56:638-646.
- Chauhan P, Osterman M, Pecht M (2012). Canary Approach For Monitoring BGA Interconnect Reliability Under Temperature Cycling. CALCE Electronic Products and Systems Center, University of Maryland, College Park, MD 20742.
- Chow WS, Leu YY, Ishak ZAM (2016). Mechanical, Thermal and Morphological Properties of Injection Molded Poly(Lactic acid)/Calcium Carbonate Nanocomposites. *Periodica Polytechnica, Mech. Eng.* 60(1):15-20.
- Gaddafi ID, Saleh TA (2017). Effects of bimetallic Ce/Fe nanoparticles on the desulfurization of thiophenes using activated carbon. *Chem. Eng. J.* 307:914-927.
- Huang X (2009). Fabrication and Properties of Carbon Fibers. *Materials* 2:2369-2403.
- Jo HS, Lee GW (2014). Thermal Expansion Coefficient and Young's Modulus of Silica-Reinforced Epoxy Composite. *Int. J. Chem. Mol. Nuclear Mater. Metallurg. Eng.* 8(11):1188-1191.
- Karadeniz ZH (2005). A numerical study on the thermal expansion coefficients of fiber reinforced composite materials. Master of Science Thesis in mechanical engineering, Energy Program, Dokuz Eylul University.
- Meszaros L, Turcsan T (2014). Development and mechanical properties of carbon fibre reinforced EP/VE hybrid composite systems. *Periodica Polytechnica, Mech. Eng.* 58(2):127-133.
- Misak HE, Sabelkin V, Mall S, Kladitis PE (2013). Thermal fatigue and hypothermal atomic oxygen exposure behavior of carbon nanotube wire. *Carbon* 57:42-49.
- Park SY, Choi HS, Choi WJ, Kwon H (2012). Effect of vacuum thermal cyclic exposures on unidirectional carbon fiber/epoxy composites for low earth orbit space applications. *Composites: Part B* 43:726-738.
- Ray BC, Rathore D (2014). Durability and integrity studies of environmentally conditioned interfaces in fibrous polymeric composites: Critical concepts and comments. Department of Metallurgical and Materials Engineering, National Institute of Technology, Rourkela-769008, India.
- Savkin A, Andronik A, Abhilash R (2015). Crack Closure Detection Using Photometrical Analysis. *Periodica Polytechnica Mech. Eng.* 59(3):114-119.
- Song K, Zhang Y, Meng J, Green EC, Tajaddod N, Li H, Minus ML (2013).

- Structural Polymer-Based Carbon Nanotube Composite Fibers: Understanding the Processing Structure-Performance Relationship. *Materials* 6:2543-2577.
- Saleh TA (2016). *Nanomaterials and polymer membranes: Synthesis, characterization, and applications*. 1st edition.
- Saleh TA (2017). *Advanced nanomaterials for water engineering, treatment, and hydraulics*. DOI: 10.4018/978-1-5225-2136-5.
- Saleh TA (2018). *Nanotechnology in oil and gas industries: Principles and applications (Topics in mining, metallurgy and minerals engineering)*. 1st edition.
- Saleh TA, Alishaheri AH, Tahir MIM, Rahman MBA, Ravooof TBSA (2017). Catalytic oxidation of cyclohexane using transition metal complexes of dithiocarbazate Schiff base. *Chem. Eng. J.* 327:423-430.
- Voicu R (2012). Structural Characterization and Mechanical Behaviour of Carbon Fiber/epoxy Composite for Aeronautical Field. *Materiale Plastice* 49(1):34-40.
- Wilkerson J, Daniel A, Daniel D (2007). Fatigue Characterization of Functionalized Carbon Nanotube Reinforced Carbon Fiber Composites. Texas A & M University, College Station, Texas 77844-3012.

A laboratory setup featuring various glassware and colored liquids. In the foreground, there are several Erlenmeyer flasks containing liquids of different colors: orange, yellow, blue, and green. A round-bottom flask with green liquid is being held by a hand in the upper left. In the background, a test tube with orange liquid is held vertically, and a larger flask with green liquid is connected to a network of red and yellow tubes. The entire scene is set against a dark background.

Journal of Chemical Engineering and Material Science

Related Journals Published by Academic Journals

- *Journal of Engineering and Technology Research*
- *International Journal of Water Resources and Environmental Engineering*
- *Journal of Civil Engineering and Construction Technology*
- *International Journal of Computer Engineering Research*
- *Journal of Electrical and Electronics Engineering Research*
- *Journal of Engineering and Computer Innovations*
- *Journal of Mechanical Engineering Research*
- *Journal of Petroleum and Gas Engineering*

academicJournals